UNIVERSITÀ DEGLI STUDI FIRENZE

DOTTORATO DI RICERCA IN SCIENZE BIOMEDICHE

CICLO XXXVI

COORDINATORE Prof. Chiti Fabrizio

How preclinical models can help to dissect the sex-related mechanisms sustaining liver disease: the role of estrogen-mediated antioxidant response in NAFLD

Settore Scientifico Disciplinare BIO/10

Dottorando

Dott. Smiriglia Alfredo

Supervisore

Prof. Morandi Andrea

Coordinatore

Prof. Chiti Fabrizio

Anni 2020 – 2023

INDEX

Abbreviations

3D: three-dimensional

AA: Activin A

AASLD: American Association for the Study of Liver Disease

ACC: acetyl-CoA carboxylase

ARE: antioxidant response elements

ASK-1: apoptosis signal regulatory kinase-1

ATCC: American Type Culture Collection

AU: Auranofin

BCA: Bicinchoninic acid

BSA: Bovine Serum Albumin

bZIP: basic leucine zipper

CAT: catalase

CD36: cluster of differentiation 36

ChREBP: carbohydrate response element-binding protein

CNC: Cap'n'Collar

CNS: central nervous system

CPT1A: carnitine palmitoyl transferase 1A

Cu: copper

CVD: cardiovascular disease

CYP: cytochrome P450

DAMPs: damage-associated molecular patterns

DGAT: diacylglycerol acyltransferase

DMEM: Dulbecco's Modified Eagle Medium

DMSO: Dimethyl sulfoxide

E2: 17β-estradiol

EASL: European Association for the Study of Liver

E-Cad: E-Cadherin

ECM: extracellular matrix

ERα: estrogen-receptor α

FASN: fatty acid synthase

FBS: fetal bovine serum

FXR: farnesoid X receptor

GDF15: growth differentiation factor 15

GLP-1: glucagon-like peptide-1

GPx: glutathione peroxidase

GR: glutathione reductase

GSH: reduced glutathione

GSSG: oxidized glutathione

HCC: hepatocellular carcinoma

HDL: high-density lipoprotein

hESC: human embryonic pluripotent stem cells

HFD: high-fat-diet

HGF: Hepatocyte Growth Factor

hiPSC: human-induced pluripotent stem cells

HLC: hepatocyte-like cells

HO-1: heme oxygenase-1

H_2O_2: hydrogen peroxide

HNF4α: Hepatocyte Nuclear Factor-4-alpha

HRP: horseradish peroxidase

IL-1β: interleukin-1β

IL-6: interleukin-6

IR: insulin resistance

KD: ketogenic diet

Keap1: Kelch-like ECH-associated protein 1

KO-DMEM: Knockout DMEM medium

KO-SR: Knockout Serum Replacement

LDs: lipid droplets

LPIAT1: lysophosphatidylinositol acyltransferase 1

LPO: lactate, pyruvate, and octanoate

MAF: musculoaponeurotic fibrosarcoma

MAPK: mitogen-activated protein kinase

MBOAT7: O-acyltransferase domain containing 7

Mn: Manganese

MS: metabolic syndrome

NADPH: nicotinamide adenine dinucleotide phosphate

NAFL: non-alcoholic fatty liver

NAFLD: non-alcoholic fatty liver disease

NASH: non-alcoholic steatohepatitis

NLRP3: nod-like receptor protein 3

NQO1: NADPH Quinone Dehydrogenase 1

Nrf2\NRF2: nuclear factor erythroid 2–related factor 2

O_2^-: superoxide anions

^-OH: hydroxyl radicals

OSM: Oncostatin M

OVX: ovariectomized

OXPHOS: oxidative phosphorylation system

PBS: Phosphate-buffered saline

PHH: primary human hepatocytes

PLIN2: perilipin 2

PNPLA3: Patatin-Like Phospholipase Domain Containing 3

PPAR: peroxisome proliferator-activated receptor

Prx: peroxiredoxins

ROCKi: Rho-associated kinase inhibitor

ROS: reactive oxygen species

SB1X: Sample Buffer 1X

SGLT2: sodium-dependent glucose transporter

SLC34A2: solute carrier family 34 member 2

SNPs: single nucleotide polymorphisms

SODs: superoxide dismutases

SREBP-1: sterol regulatory element-binding protein-1

T2DM: type II diabetes mellitus

TCA: tricarboxylic acid cycle

TGF-β: transforming growth factor-beta

TH: thyroid hormones

TLRs: toll-like receptors

TM6SF2: transmembrane 6 superfamily member 2

TNFα: tumor necrosis factor α

TR: thyroid hormone receptor

Trx: thioredoxins

Trx2: thioredoxin-2

TrxR: thioredoxin reductase

TXNIP: thioredoxin interacting protein

VitC: vitamin C

VitE: vitamin E

VLDL: very low-density lipoproteins

wnt3a: Wingless-Type MMTV Integration Site Family, Member 3 A

Zn: zinc

1. Morphology and functional organization of liver tissue

The liver is the largest gland of the body accounting for approximately 2% of an adult's body weight. A peculiar characteristic of this organ is its double vascularization. In addition to the hepatic artery, it is also supplied by the portal vein. This peculiarity makes the liver an organ of first passage receiving blood from the splanchnic circulation, which is rich not only in nutrients but also in toxic substances and microbiological agents present in the gastrointestinal tract [1]. The liver is a mixed gland, with both endocrine and exocrine functions: endocrine functions include the secretion of numerous hormones participating in the metabolism of lipids, proteins, and carbohydrates, in iron homeostasis and body development. Furthermore, this organ secretes the vast majority of serum proteins, in fact the major exocrine function is bile secretion [2] [3].

From a histological point of view, the basic architectural and functional unit of the liver is the lobule. Liver lobules are roughly hexagonal with each of six corners demarcated by the presence of a portal triad of vessels consisting of a portal vein, bile duct, and hepatic artery. Microscopic analysis of the liver lobule allows us to easily identify the parenchymal component, the hepatocytes, which appear as large polyhedral cells, often multinucleated. Specific histological stains facilitate the recognition of different non-parenchymal cell types, which we can be divided into resident cells, such as Kupffer, stellate and sinusoidal epithelial cells, and cells of blood origin, such as NK, B, and T lymphocytes.[4].

2. Hepatic disease: non-alcoholic fatty liver disease (NAFLD)

Since the liver has a crucial role in normal physiological processes, liver diseases such as fibrosis, cirrhosis, and hepatocellular carcinoma (HCC), result in systemic homeostasis disruption and lead to high rates of morbidity and mortality. Globally, liver disease accounts for 2 million deaths annually and is responsible for 4% of all deaths (1 out of every 25 deaths worldwide), which are largely attributable to complications of cirrhosis and HCC [5]. In particular, cirrhosis currently causes 1.16 million deaths, and liver cancer accounts for 788,000 deaths worldwide, making them the 11^{th} and 16^{th} most common causes of death, respectively, each year.

The most common causes of chronic liver disease are related to viral hepatitis and non-alcoholic fatty liver disease (NAFLD [6].

NAFLD term can be referred to a broad spectrum of histological liver changes spanning from the more benign condition of non-alcoholic fatty liver (NAFL) to the more severe condition namely non-alcoholic steatohepatitis (NASH): in particular, NAFL consists of hepatic steatosis without inflammatory manifestation, whereas NASH is a form of hepatic steatosis associated with lobular inflammation, hepatocyte injury (leading to the so-called “ballooning” phenotype and necrosis) and apoptosis that can ultimately lead to fibrosis and cirrhosis [7, 8]. End-stage of this disease process is represented by the development of HCC (Figure 1) however, the majority of NAFLD patients do not progress to the neoplastic form but a portion of NAFLD patients develop NASH, which is associated with liver failure and HCC [9]. NAFLD is strongly associated with many of the features that characterize metabolic syndrome (MS), such as systemic hypertension, dyslipidemia, insulin resistance (IR), and type II diabetes mellitus (T2DM) [10].

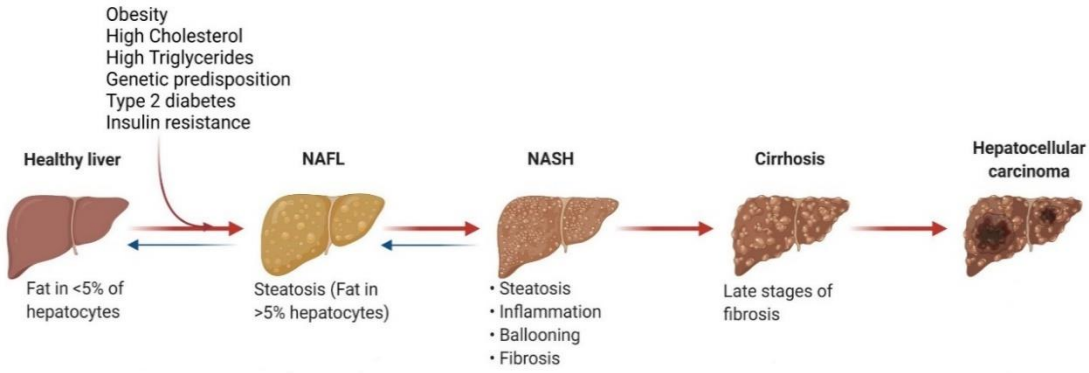

Figure 1. Progression stages of NAFLD until the HCC [11].

2.1 **Epidemiology, prevalence, and sex difference**

NAFLD affects a quarter of the global adult population with a global prevalence estimate of around 32.4% [12]. However, there are remarkable geographical and ethnic differences in the NAFLD prevalence rates [13]; indeed, the prevalence of NAFLD is highest in the Middle East, South America [14], and Western European countries [15] (Figure 2). In a recent analysis, it was estimated that there are 64 million people in the United States and 52 million people in 4 European countries (Germany, France, Italy, and the United Kingdom) potentially affected by NAFLD [16]. A large part of the worldwide increase in NAFLD is driven by overweight and obesity, a global issue whose incidence has doubled in the last decade [17].

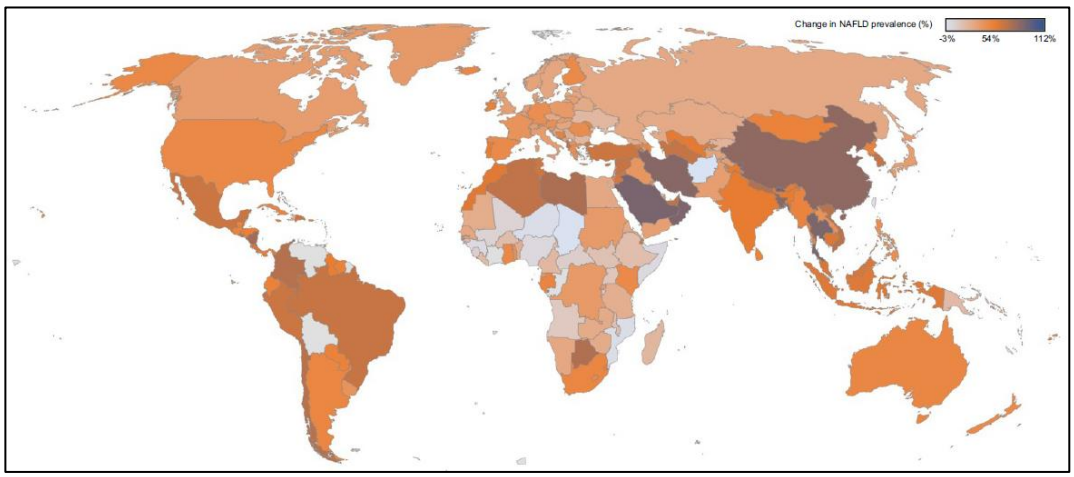

Figure 2. Global heat map of changing NAFLD prevalence [13].

An important aspect regarding NAFLD incidence emerged from longitudinal studies that suggest a higher incidence in the male sex as compared to the female [18, 19]. Men commonly display an increased prevalence of NAFLD during adulthood from young to middle-aged, which starts declining after the age of 55 years [20, 21]. In women of fertile age, the prevalence of NAFLD is lower than in men owing to the putative protective effect of estrogens which, indeed, wanes after menopause. Accordingly, the prevalence of NAFLD in women rises after the age of 50 years, peaks at the age between 60 and 69 years, and declines after 70 years [20-22]. As a result of this, post-menopausal women compared to men of the same age have a similar [23] or even higher prevalence of NAFLD. In agreement with these findings, an Italian multicentric study on 5408 healthy women who had hysterectomies, randomly assigned to receive tamoxifen, an estrogen inhibitor, or placebo for 5 years, showed that tamoxifen was associated with a higher risk of development of NAFLD/NASH

especially in overweight/obese women [24], thus suggesting estrogens as a protective factor for the development of NAFLD.

Finally, in accordance with the dramatic increase in the global incidence of metabolic risk factors and the aging population, it is expected that the burden of advanced NAFLD manifestations will more than double in the next decade. Notably, metabolic risk factors in children and teenagers constitute one of the biggest threats to global health in the coming decades [25].

2.2 **Pathogenesis and molecular mechanism**

Since NAFLD is a heterogeneous pathology, the underlying mechanism for the development and progression of disease is complex and multifactorial. Over the years, the first pathological hypothesis formulated consists in the synergic action of "*two hits"*: in particular, hepatic fat accumulation secondary to hyper-caloric diets, a sedentary lifestyle, and obesity, acts as the *"first hit"*, sensitizing the liver to further insults acting as a *"second hit"*, which can activate inflammatory cascades and fibrogenesis [26]. Although this hypothesis is supported by mouse models of obesity where, following the "*second hits"*, inflammation and fibrogenesis are observed [27], this is a simplified view for a complex disease such as NAFLD. Consequently, a "*multiple-hit hypothesis"* has substituted the outdated "*two-hit hypothesis"* for the progression of NAFLD. In addition to lipid accumulation and inflammation, other factors involved in NAFLD development are IR and changes in the intestinal microbiome. IR results in increased hepatic *de novo* lipogenesis and impaired inhibition of adipose tissue lipolysis, with consequent increased net flux of fatty acids to the liver [28]. IR also promotes adipose tissue dysfunction with consequent altered production and secretion of adipokines and inflammatory cytokines [29]. Moreover, consequently, due to excessive hepatic lipid accumulation, mitochondrial dysfunction with the production of reactive oxygen species (ROS), and endoplasmic reticulum stress can occur and lead to reversible or irreversible cell damage [30]. Another tissue that may contribute to "*multiple-hit hypothesis"* is the bowel. Indeed, when bowel permeability is increased, a phenomenon that may be linked also to altered microbiota, the absorption of fatty acids can be enhanced in parallel leading to an increase in circulating levels of inflammatory molecules [31].

Overall, these hepatic insults can lead to hepatocyte death or activation of hepatic stellate cells with deposition of the fibrous matrix, to develop fibrosis, and lastly cirrhosis and HCC. Although the dogma states that steatosis always precedes inflammation, it is now recognized that NASH can be the initial liver lesion: the timing and combination of genetic, external, and intracellular events rather than the simple

sum of hepatic insults result in different pathways that lead to NAFL or NASH, respectively [32].

2.2.1 Fat accumulation

The fundamental defect in the first steps to the development of NAFLD disease is impairment in insulin sensitivity, which has a potent action to suppress adipose tissue lipolysis resulting in large changes in plasma fatty acid concentration [33]. Free fatty acids are bound by albumin and delivered to the liver where, through fatty acid transport proteins, such as the cluster of differentiation 36 (CD36), can enter into the hepatocytes [34]. In addition to the amount of free fatty acid derived from lipolysis of the adipocytes that accounts for approximately 60%, lipids can be derived from *de novo* lipogenesis using glucose or fructose [35]. Hepatic lipogenesis can be increased by activation of transcription factors such as sterol regulatory element-binding protein-1 (SREBP-1), carbohydrate response element-binding protein (ChREBP), and peroxisome proliferator-activated receptor (PPAR)-γ [36]. Moreover, diet also contribute to the hepatic free fatty acid pool. In fact, obesity is the main risk factor for NAFLD, and studies in obese subjects indicated that increased consumption of carbohydrates and saturated fats contribute to lipid accumulation in NAFLD [37].

The predominant fate of free fatty acid in the liver is to either undergo mitochondrial β-oxidation or be esterified in the endoplasmic reticulum to form triglycerides: in particular, under insulin resistance states, β-oxidation of free fatty acid is inhibited, thus promoting hepatic lipids accumulation [38]. In particular, triglycerides accumulated into lipid droplets (LDs), dynamic and metabolically active organelles that consist of a hydrophobic core of neutral lipids (cholesterol esters and triglycerides) enveloped by a phospholipid monolayer. The hydrolysis of LDs produces lipid metabolites that affect cell homeostasis, inducing organelle dysfunction, cell injury, cell malfunction, and death [39]. In fact, aberrant lipolysis of these LDs is involved in NASH progression (Figure 3).

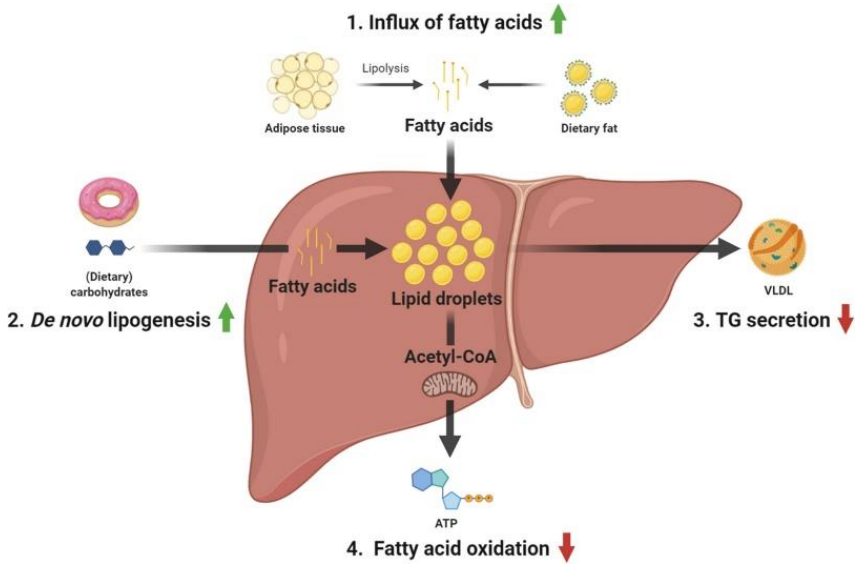

Figure 3. Overview of the main pathways contributing to triglyceride accumulation in NAFLD [40].

2.2.2 **Oxidative stress**

Oxidative stress occurs when the balance between oxidant and antioxidant mechanisms is disrupted, leading to the accumulation of highly reactive molecules or free radicals namely ROS, which include oxygen-derived molecules with one or more unpaired electrons or as non-radical species. The major physiologically relevant ROS are superoxide anions ($O_2^{\cdot-}$), hydroxyl radicals ($^{\cdot}OH$), and hydrogen peroxide (H_2O_2) that could be produced in differential cellular compartments. Under homeostatic conditions, ROS production is buffered by antioxidant systems that reduce ROS-induced oxidative damage; instead, the increase in ROS levels has harmful effects on several cellular macromolecules (DNA, lipids, proteins, etc.) thus leading to the accumulation of damaged cellular components [41]. Therefore, the alteration of the cellular redox balance is a risk factor for the development of various pathologies.

The main role of mitochondria is to generate ATP via oxidative phosphorylation system (OXPHOS), through five protein complexes and two electron transporters embedded into the inner mitochondrial membrane [42]. Indeed, ATP production is achieved by coupling electron transfer to proton translocation across the inner mitochondrial membrane, resulting in the formation of an electrochemical gradient, which generates a driving force that drives ATP synthesis by the fifth complex, namely ATP synthase. During cellular respiration, electrons are transferred from the tricarboxylic acid cycle (TCA) products, NADH and $FADH_2$, via complexes I and II, respectively, to the ubiquinone. They then pass through complex III and cytochrome C, ending in complex IV, which reduces O_2 to H_2O [43]. During this process, electrons

can escape transfer between the OXPHOS complexes and partially reduce O_2 to O_2^-, which is the main ROS produced at the mitochondrial level. Under physiological conditions, however, ROS scavenging mechanisms rapidly convert O_2^- into H_2O_2, which is then transported out of the mitochondria. In contrast, under pathological conditions, excessive ROS production or inefficient scavenging mechanisms cause an excessive increase in ROS levels, favoring oxidative stress [44] [45].

During NAFLD progression, due to a high fatty acid intake or a condition of IR, increased mitochondrial fatty acid oxidation and TCA activity provide reducing equivalents to OXPHOS [46]. The uncoupling between β-oxidation, TCA cycle, and OXPHOS results in inefficient lipid metabolism and ROS overproduction in the mitochondria during NAFLD progression [47]. The increase of oxidative stress can also lead to lipid peroxidation, and the production of reactive metabolites such as malondialdehyde and 4-hydroxynonenal [48, 49]. In addition, the end-products of lipid peroxidation are known pro-inflammatory mediators that can activate stellate cells and lead to collagen production and ultimately to liver fibrosis [50].

2.2.3 Inflammation and fibrosis

Inflammation is considered the key mechanism of NAFLD progression and can be triggered by extrahepatic (e.g., adipose tissue) and intrahepatic (e.g., lipotoxicity, oxidative stress, and cell death) factors [51]. Adipose tissue dysfunction can lead to the production of cytokines by liver macrophages in visceral adipose tissue, including tumor necrosis factor α (TNFα), interleukin-1β (IL-1β) and IL-6 causing liver damage and promoting impaired insulin signaling. Moreover, increased free fatty acid uptake by hepatocytes can induce lipotoxicity and subsequent cell death, which accentuate liver inflammation [52, 53].

Kupffer cells, specific liver macrophages, contribute to the inflammation through both cytokines production and by increasing the activation of inflammasome components, namely nod-like receptor protein 3 (NLRP3) [54]. The NLRP3 inflammasome can be activated by multiple ligands for example stress signaling molecules namely damage-associated molecular patterns (DAMPs), released following hepatocyte injury induced by lipid excess [55]. Kupffer cells detect DAMPs, triggering their activation and the release of proinflammatory mediators and thus could be involved in NASH development [56]. Finally, also oxidative stress and translocated bacterial products can activate Kupffer cells via toll-like receptors (TLRs), particularly TLR4, resulting in increased TNFα and IL-1β production, a mechanism shown to participate in NASH in animal models [57].

Lipid accumulation, oxidative stress production, and inflammation define the characteristic overview of NASH, which can progress to fibrosis following liver damage. An overactive inflammatory response can result in liver dysfunction and lead to the deposition of fibrotic tissue in parallel to cell death. Liver fibrosis consists of the altered formation of extracellular matrix (ECM) which leads to an excessive deposit of extracellular proteins, including several distinct types of fibrillar and non-fibrillar collagens, produced and released by hepatic stellate cells [58, 59].

2.3 Risk factors and clinical features

According to the "*multiple hits hypothesis*", NAFLD has a multifactorial pathogenesis and consequently the risk factors that play a role in the development of the disease are numerous. Genetic factors especially in the form of single nucleotide polymorphisms (SNPs) for specific genes, could play a major role. The most important SNP is I148M variant of *Patatin-Like Phospholipase Domain Containing 3* (PNPLA3) gene, located on the long arm of chromosome 22, which consists in the substitution of guanine in place of a cytosine (rs738409), which results in isoleucine to methionine conversion [60, 61]. PNPLA3 gene is responsible for the production of an intracellular lipase named adiponutrin, an enzyme implicated in the hydrolysis of triglycerides inside the adipocytes [62]. The mechanism by which the I148M variant induces the development of steatosis in humans seems related to the deposition of the mutated protein that is associated with decreased secretion of very low-density lipoproteins (VLDL) from the liver and subsequent intracellular lipid accumulation in the hepatocytes [63].

Another relevant SNPs is the substitution of a cytosine by a thymine (rs58542926) in the transmembrane 6 superfamily member 2 (TM6SF2) gene, resulting in a conversion of lysine to glutamate at residue 167 (E167K), with a decrease of approximately 50% of the protein functionality. Consequently, TM6SF2 polymorphism determines lower plasma levels of VLDL with subsequent lipid accumulation in hepatocytes [64, 65]. Finally, polymorphism in the *O-acyltransferase domain containing 7* (MBOAT7) gene is associated with a reduced function of the encoded protein, namely lysophosphatidylinositol acyltransferase 1 (LPIAT1). A reduction of LPIAT1 expression correlates with increased triglyceride synthesis and accumulation in hepatocytes [66].

In addition to genetic factors, clinical features have an important role in NAFLD development. In fact, since obesity and T2DM are conditions associated with IR, overweight and diabetic persons have elevated risk of developing NAFLD [67]. Therefore, the prevalence of NAFLD is higher in individuals with metabolic syndrome

and, moreover, the presence of multiple traits of metabolic syndrome is associated with a higher likelihood of more severe liver diseases [68]. Moreover, in non-diabetic subjects, NAFLD prevalence is higher in the presence of cardiovascular disease (CVD), supporting the hypothesis that there is a relationship between NAFLD and CVD, independently of other comorbidities [69].

Finally, environmental factors such as dietary habits and physical activity play an important role in the pathogenesis of NAFLD. Studies focusing on the nutritional behavior of NAFLD patients showed an increased consumption of foods characterized by a low nutritional content and high sodium and animal fats consumption. In addition to these dietary habits, it has been documented that individuals with NAFLD are less physically active and more sedentary than healthy individuals [70].

3. Treatment approaches against NAFLD

Despite the high prevalence of NAFLD and its increasing impact on global health, there are currently no approved treatments for NAFLD, although the understanding of the epidemiology and pathophysiology of the disease and the identification of therapeutic targets are a common goal for the research community [71]. Therefore, similar to the recommended treatment for MS, lifestyle modifications including weight loss, increased physical activity, and dietary changes are considered as a first-line intervention for the treatment of NAFLD [72]. Alternatively, weight loss through bariatric surgery, even with rapid weight reduction after surgery, is largely focused on subsets of patients with severe obesity and progressive NAFLD [73].

Although lifestyle interventions have been shown to improve NAFLD, those approaches are unlikely to be curative; therefore, since NAFLD is a multifactorial disease related to MS, the optimal therapeutical strategy consists of a multidisciplinary approach aiming at targeting features related to the pathological processes that drive disease progression (Figure 4).

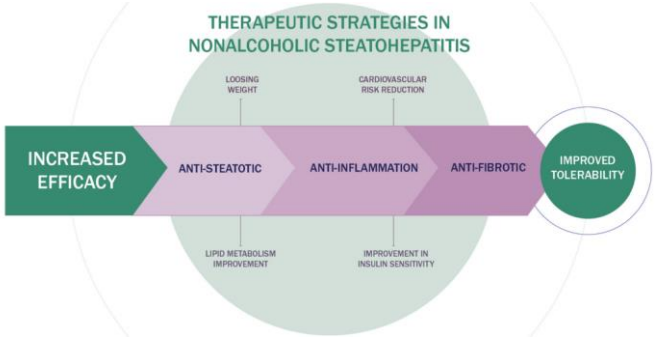

Figure 4. Therapeutic algorithm for NAFLD treatment [74].

3.1 Diet and lifestyle

Most patients with NAFLD consume high-calorie foods with elevated content of saturated fat and cholesterol and less polyunsaturated fatty acids than healthy persons. Therefore, as recommended by both the European Association for the Study of Liver (EASL) and the American Association for the Study of Liver Disease (AASLD) guidelines, diet and lifestyle changes represent an important part of the management of NAFLD [75]. In fact, the standard guidelines for dietary changes recommend reducing the intake of saturated fat to <7% of total calories and maintaining dietary cholesterol intake at <200 mg/day and total fat at 25% to 35% of total calories [76]. A widely used nutritional model for patients with NAFLD is the Mediterranean diet, which is beneficial in the prevention and management of multiple metabolic conditions, including CVD and diabetes [77]. Mediterranean diet, characterized by a high intake of olive oil, unrefined cereals, fruit, pulses, vegetables, fish and a low intake of red meat, sweets and alcohol, leads to a reduction in hepatic steatosis with an increase in insulin sensitivity, compared with a low-fat-high-carbohydrate diet, in NAFLD patients [78].

Further beneficial improvements in NAFLD patients have been observed by combining a healthy diet with frequent physical activity: current guidelines recommend around 150 minutes/week of moderate exercise [79]. In fact, there are several publications regarding the benefits of exercise in NAFLD patients: regular aerobic physical activity led to a reduction of incidence risk of 35% for diabetes and 49% for CVD [80] and an improvement in both liver tissue inflammation and fibrosis [81].

Therefore, following a proper diet combined with moderate physical activity may represent a valuable strategy for reducing the development and progression of NAFLD.

3.2 Targeting *de novo* lipogenesis and hepatic lipid metabolism

Since lipid accumulation is considered an essential step in the progression of the disease, targeting the abnormal lipid metabolic mechanisms to prevent liver fat accumulation appears to be a promising therapeutic approach [82].

The transcription factors belonging to the nuclear hormone receptor superfamily, called PPARs, which are considered key regulators of fatty acid metabolism in liver and adipose tissue are among the main candidates to be targeted [83]. There are three different subtypes of PPARs, designated as α, β/δ, and γ, which exert pleiotropic functions in different tissues mainly related to metabolism and immunity. Given the link between the different forms of PPAR, lipid metabolism, and liver disease, these molecular players are considered potential therapeutic targets in NAFLD [84, 85].

Among the most important drugs used is Pioglitazone, a PPARγ agonist that increases the plasma levels of adiponectin, a cytokine produced by adipocytes (also called adipokine) that induces fatty acids β-oxidation in liver and muscles [71, 86]. In this way, Pioglitazone leads to a reduction in hepatic triglyceride content homeostasis and insulin sensitivity [87]. The therapeutic effect of Pioglitazone is currently tested in a phase 4 clinical study (NCT00994682) and AASLD and EASL guidelines recommend the use of Pioglitazone in patients with NASH [75, 79]. Another drug is Saroglitazar, a PPARα agonist able to induce β-oxidation improving liver fat content, and insulin resistance in patients with NAFLD [88]. Similarly to PPARs, farnesoid X receptor (FXR) is a crucial molecular actor in the expression of hepatic genes involved in bile acid metabolism, but also in lipid synthesis and transport. FXR activation can affect hepatocyte lipid balance, inactivating *de novo* lipogenesis mediated by SREBP-1c but also inhibiting CD36 and lipogenesis enzymes [89]. Due to the FXR activation effect on lipid metabolism, FXR agonists could represent a therapeutic option for NAFLD. In fact, Ma *et al*. showed that a knockout mouse model for Fxr gene ($Fxr^{-/-}$ mice) spontaneously developed hepatic steatosis with elevated levels of free fatty acids and IR. Interestingly, when treated with an FXR agonist, $Fxr^{-/-}$ mice were able to restore normal triglyceride levels within the liver [90, 91]. FXR agonists are divided into steroidal and non-steroidal: obeticholic acid is a selective steroidal agonist currently in a phase 2, randomized, placebo-controlled study (NCT02633956). Treatment with obeticholic acid improved hepatic steatosis and fibrosis in NAFLD patients [92]. In addition, several other FXR agonists are currently under phase 2/3 trials, including cilofexor and tropifexor. In NASH bearing animal models and NASH bearing patients, tropifexor reduced lipid content and fibrosis inflammatory markers [93]. Among the new FXR agonists, EDP-305 and vonafexor have already been employed in clinical trials with favorable results, mainly displaying a reduction in liver fat content [94, 95].

Fat exacerbation can lead to an accumulation and production of lipotoxic metabolites, thereby damaging the hepatocytes. Therefore, to avoid this, a possible therapeutic strategy is to target *de novo* liver lipogenesis, which may be upregulated by 20-30% in patients with NAFLD compared to healthy controls [96]. Fatty acid synthase (FASN) is the rate-controlling enzyme that uses malonyl-CoA to produce palmitic acid in the *de novo* lipogenesis pathway. FASN expression is significantly higher in patients with NAFLD and treatment with TVB-2640, a FASN inhibitor tested in a phase 2 clinical trial (NCT03938246), showed promising results in patients with NASH with respect to normal subjects [97].

Acetyl-CoA carboxylase (ACC) enzyme, which converts acetyl-CoA to malonyl-CoA, represents an additional target related to *de novo* lipogenesis [98]. A preclinical study demonstrated that GS-0976 drug (Firsocostat), an ACC inhibitor currently being evaluated in a phase IIb (NCT03449446), decreased hepatic steatosis and fibrosis-related markers in a rat choline-deficient, high-fat-diet (HFD) NAFLD model [99]. Moreover, administration of GS-0976 for 12 weeks suppressed hepatic lipid synthesis while simultaneously increasing β-oxidation in non-cirrhotic patients with NASH [100]. Finally, since LDs formation is the most important event in NAFLD, targeting enzymes involved in this process could be a potential therapeutic option. Diacylglycerol acyltransferase (DGAT) enzyme catalyzes the last step in triglyceride formation, esterifying the diacylglycerol with a third fatty acid [101]. Two isoforms of DGAT exist with different tissue-expression: a selective inhibitor of the DGAT2 isoform decreased lipidic hepatic accumulation in HFD-fed mice models [102].

3.3 Antioxidant stress agents

During NAFLD progression, increased lipid peroxidation is associated with the decrease of the hepatic antioxidant properties. Therefore, several antioxidants have been studied experimentally and clinically against NAFLD patients [103]. Antioxidants are substances that inhibit the oxidation of any biomolecule, neutralizing the harmful effects of oxidation caused by free radicals, particularly ROS [104].

One of the most important enzymatic antioxidant defenses is the system orchestrated by the nuclear factor erythroid 2–related factor 2 (Nrf2), a transcriptional factor that controls the expression of many detoxifying enzymes [105]. Nrf2 liver expression is downregulated in patients with NAFLD and Nrf2 deficient-murine models [106, 107] are more susceptible to diet-induced steatosis and inflammation [108]. Therefore, impairing Nrf2 activation is currently being investigated as NAFLD potential therapy. Oltipraz, a Nrf2-inducing synthetic compound, significantly reduced hepatic fibrosis in rats fed on a choline-deficient L-amino acid-defined diet, a model of NAFLD [109]. The efficacy and safety of oltipraz administration in patients with NAFLD were verified in the phase 2 clinical trials (NCT01373554 and NCT00956098). NCT01373554 revealed that 24-week treatment of oltipraz significantly reduced the liver fat content in a dose-dependent manner in patients with NAFLD [110].

Moreover, natural compounds such as resveratrol and hesperetin have also been reported as Nrf2 modulators. In particular, resveratrol treatment reversed palmitic acid-induced mitochondrial oxidative stress-mediated steatosis in HepG2 cells [111]. In addition, resveratrol decreases oxidative stress in NASH-bearing mice by increasing the regulation of antioxidant systems [112]. Clinically, resveratrol

administration for 12 weeks significantly improved liver inflammation and hepatic fibrosis in NAFLD patients [113]. On the same line, hesperetin, a natural compound abundant in oranges and lemons, was able to increase the Nrf2 pathway alleviating lipid deposition and oxidative markers in oleic acid-induced HepG2 cells [114]. The safety of the clinical use of Nrf2 inducers in advanced cases of NASH is still a matter of debate. In fact, although the activation of the Nrf2 pathway is associated with the improvement of NASH, it is also activated during liver carcinogenesis, both in animal models and in humans.

More antioxidant compounds that could be relevant in the pathology are vitamin C (VitC) and vitamin E (VitE), which dietary intake has demonstrated to improve the detoxifying system in NAFLD patients [115]: in particular, VitE supplementation, a lipid-soluble vitamin stored in the liver and fat tissue, has reduced oxidative damage and intrahepatic lipid accumulation in HFD-fed mice [116]. Currently, VitE is supplemented in NASH patients, associated with reduced serum hepatobiliary enzymes and hepatic steatosis but without improvement of liver fibrosis [117]. A phase 3 clinical trial (NCT00063622) showed that VitE supplementation, alone or in combination with pioglitazone, reduced hepatic steatosis and lobular inflammation when compared to the placebo group [118].

In addition to VitE, other antioxidants are currently being studied for the treatment of NAFLD: for example, carotenoid beta-cryptoxanthin compound prevented the progression of steatosis and fibrosis in NASH mice fed a high-cholesterol and high-fat diet [119].

Finally, since T2DM is closely associated with NAFLD, the antidiabetic drug metformin has been proposed to ameliorate NAFLD features and clinical parameters. Several studies showed that metformin can protect against liver damage by lowering the increased serum cholesterol and consequently hepatic steatosis in HFD-fed mice [120]. Moreover, metformin protected against palmitate-induced apoptosis in primary rat hepatocytes and HepG2 cells [121]. Therefore, metformin may be useful in the prevention and/or treatment of NAFLD, and its beneficial effects might in part be related to reduced disease markers.

3.4 Targeting inflammation and fibrogenesis

Increasing evidence shows that NLRP3 inflammasome is a central driver of inflammation during NAFLD progression [122]. Therefore, pharmacological inhibition of NLRP3 activation has been proposed for a potential therapeutic approach: sulforaphane is an NLRP3-suppressor molecule able to reduce hepatic disease indicators, such as total cholesterol plasma levels and free fatty acids levels, in mice

fed with an HFD [123]. Moreover, oral administration of sulforaphane restored mitochondrial function and suppressed NLRP3 in NAFLD-bearing mice [124]. A second study showed that MCC950, an inflammasome block-selective small compound, significantly decreased infiltration of inflammatory cells and fibrosis in experimental NASH murine models [54]. An additional approach consists of targeting the cytokine-production that occurs during the inflammatory process. Pentoxifylline is a methylxanthine derivative able to decrease TNFα gene expression, which showed beneficial effects in weight loss, improving liver function and histological changes in NAFLD patients [125]. Infliximab, a TNFα inhibitor, was able to slightly reverse the NASH histopathological score and was effective on inflammation and fibrosis-related traits in the NASH-bearing rats [126]. Many other anti-inflammatory approaches have been proposed: for instance, blocked inflammatory macrophage activation by interfering with the TLR pathway, especially TLR4 isoform, through the use of inhibitor serelaxin showed an increase in the antifibrotic effect of rosiglitazone, a PPARγ agonist, in a fibrotic mice model [127]. In this way, liver fibrosis represents another process to control or reverse in NAFLD targeting approaches.

Similar to cytokines, galectin 3 is a β-galactoside binding protein associated with chronic inflammation and fibrogenesis and secreted by macrophages upon liver injury in NASH [128]. Belapectin (GR-MD-02), an inhibitor of galectin 3, reduced hepatic fibrosis and portal hypertension in rats and its efficacy was verified in 162 patients with NASH, cirrhosis, and portal hypertension (NCT02462967) [129]. Another significant player in NAFLD fibrosis is the transforming growth factor-beta (TGF-β) protein, which causes hepatocytes' apoptosis and differentiation of hepatic stellate cells into extracellular matrix-secreting myofibroblast. TGF-β signaling can be targeted using specific drugs, e.g., the TGF-β receptor inhibitors galunisertib and oxy210, that effectively ameliorated hepatic fibrosis and liver inflammation in both human and mice [130, 131].

Finally, inhibiting migration and activation of hepatic stellate cells with the antifibrotic agent cenicriviroc, reduced fibrosis traits without worsening of NASH associated symptoms in 20% of patients compared to 10% for placebo after 1 year of treatment [132].

3.5 **Antidiabetic drugs**

Since NAFLD is a metabolic-related liver disease with significant link with obesity and T2DM, numerous anti-diabetic agents have tested as therapeutic approaches in experimental models and NAFLD patients, showing some beneficial effects. Glucagon-like peptide-1 (GLP-1) is an endogenous hormone that directly stimulates insulin production and release [133], and its levels are decreased in NAFLD patients [134]. Indeed, GLP-1 agonists, approved for T2DM therapy, have demonstrated a reduction of hepatic steatosis and markers of liver damage in NAFLD induced diabetic mice [135]. In particular, the treatment with Liraglutide, a GLP-1 receptor agonist, in NAFLD patients reduced metabolic dysfunction and lipotoxicity compared to the placebo group [136]. Another GLP-1 receptor agonist is Semaglutide, which improved in fibrosis in patients with NASH [137]. Sodium-dependent glucose transporter (SGLT2) is primarily expressed in the proximal tubule epithelium of the kidney and is responsible for kidney-glucose reabsorption and SGLT2 inhibition is considered as a new antidiabetic approach [138]. Moreover, several studies have shown that SGLT2 inhibition, significantly reduced levels of liver enzymes, steatosis, hepatocyte damage, and fibrosis in patients with NAFLD and T2DM [139].

3.6 **Thyroid hormone receptor agonists in the treatment of NAFLD**

The thyroid hormone receptor (TR) system plays a crucial role in regulating metabolic homeostasis of the liver since, following the binding to thyroid hormones (TH) and subsequent TR activation, it can modulate the expression of genes involved in lipid metabolism, influencing processes such as lipogenesis, lipolysis, and fatty acid oxidation [140]. TH receptor β (TR-β) is the most abundant TR isoform in the liver but is also expressed in other tissues. Activation of hepatic TR-β is associated with systemic lipid-lowering, increased bile acid synthesis, and fat oxidation [141].

Given the functions of the TR system in metabolic and energy homeostasis of the liver, disruption in the normal TH signaling has been implicated in the pathogenesis of NAFLD and its expression in the liver is reduced in patients with NASH [142].

Preclinical studies utilizing TR agonists, especially for TR-β, have shown promising outcomes, including reductions in hepatic steatosis, inflammation, and fibrosis [143]. Among these selective TR-β agonists, GC-1, formerly known as Sobetirome, is the first TR-β agonist that has been generated and then has served as a scaffold compound for the development of subsequent derivatives. Sobetirome administration can reduce triglyceride and cholesterol content preventing hepatic steatosis in rats placed on HFD [144, 145]. The reduction in hepatic triglycerides was accompanied by a concomitant decrease in lipoperoxidation [146]. Moreover, Sobetirome

ameliorated hepatic steatosis also in other animal experimental models, such as ob/ob mice and Western diet-fed mice [145].

Another promising TR-β agonist for the management of NAFLD is Resmetirom, which has been shown to effectively impair lipid accumulation and inflammation in an *in vitro* model of NAFLD and preclinical models of diabetes and obesity [141, 147]. Clinical trials have also shown encouraging results, with Resmetirom demonstrating improvements in liver function and metabolic parameters in patients with NAFLD, such as reduction in hepatic lipid fraction, circulating cholesterol and triglycerides, and a higher rate of NASH resolution, compared to placebo [148-150]. Despite these promising findings, there is a need for further investigation to elucidate the precise mechanisms of action of Resmetirom, optimize dosing strategies, and evaluate long-term safety and efficacy outcomes.

4. **Scavenging ROS systems**

In addition to dietary non-enzymatic antioxidants, which usually prevent or attenuate oxidative damage, human cells present an important enzymatic antioxidant defense armamentarium. As anticipated in the previous paragraph, the main cellular antioxidant mechanism is driven by Nrf2, a member of the Cap'n'Collar (CNC) basic leucine zipper (bZIP) family of transcription factors [151]. Under normal conditions, Nrf2 is localized in the cytoplasm and sequestered by its inhibitor, Kelch-like ECH-associated protein 1 (Keap1). Keap1 acts as a sensor for oxidative stress and determines the degradation of Nrf2 by proteasome via E3 ubiquitin ligase [152]. During exposure to free radicals or oxidative stress, Keap1 becomes oxidized at critical cysteine residues disrupting the E3 ubiquitin ligase system and leading to conformational changes in the Keap1–Nrf2 complex. As a result, Nrf2 escapes Keap1 control and translocates to the nucleus, where it dimerizes with small musculoaponeurotic fibrosarcoma (MAF) protein and binds to the antioxidant response elements (ARE) present in the promoter regions of target antioxidant genes [153] (Figure 5). Among the several antioxidant enzymes activated by Nrf2, the principals are heme oxygenase-1 (HO-1), NADPH Quinone Dehydrogenase 1 (NQO1), and also superoxide dismutases (SODs), catalase (CAT), and thioredoxins (Trx) [154].

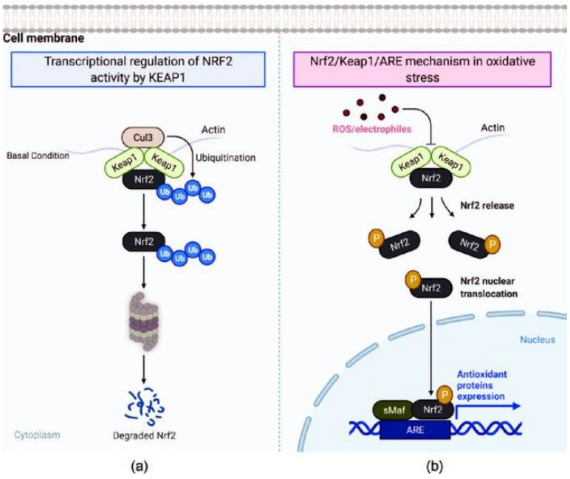

Figure 5. Schematic of Nrf2 pathway under normal (a) or oxidative (b) conditions [155]

SODs are metalloenzymes that rely on a metal cofactor for their activity and present two isoforms with different cellular localization, namely cytoplasmic SOD1 and mitochondrial SOD2. SOD1 utilizes copper (Cu) and zinc (Zn), while SOD2 uses manganese (Mn) as cofactors [156]. Specifically, SODs catalyze the dismutation of superoxide anion free radical O_2^- into molecular oxygen and H_2O_2 and decrease O_2^- levels which can damage the cells at excessive concentration [157]. Several studies showed that SODs and reduced glutathione (GSH) expression is decreased in NAFLD patients [158, 159], suggesting the use of chemical compounds to activate these antioxidant mechanisms to counteract NAFLD progression.

A further antioxidant enzyme that can also be activated by Nrf2 is glutathione peroxidase (GPx), an enzyme containing a seleno-cysteine residue involved in the regulation and modulation of cellular redox homeostasis. This enzyme is responsible for maintaining the supply of GSH, the oxidation of which into oxidized glutathione (GSSG) allows the reduction of H_2O_2 to H_2O and more in general is a ROS buffering system. Finally, GSSG must be converted back to its reduced form to be able to foster ROS scavenging, a mechanism dependent on nicotinamide adenine dinucleotide phosphate (NADPH) and the enzyme glutathione reductase (GR) [160].

Finally, among endogenous antioxidant systems responsible for ROS detoxification, an important role could be mediated by the Trx enzyme, promoting the conversion of H_2O_2 to H_2O and molecular oxygen [161]. Trx system is an important antioxidant reduction mechanism closely related to cell proliferation, differentiation, and tumor progression, removing excessive ROS and maintaining the intracellular redox balance.

4.1 Thioredoxin (Trx) antioxidant mechanism

Trx is an important antioxidant molecule involved in cellular redox-dependent regulation that together with thioredoxin reductase (TrxR) enzyme and NADPH, compose the ubiquitous disulfide oxidoreductase antioxidant Trx system. Trx is a small multi-functional protein that plays a crucial role in cellular redox regulation and signaling in normal and tumor cells. Structurally, Trx has a redox active site composed of two residues of cysteine (Cys-Gly-Pro-Cys), which form a reversible disulfide bridge [162, 163]. In mammalian cells, two isoforms of Trx have been characterized with different intracellular localization: Trx1 in the cytoplasm, Trx2 in the mitochondria. Although Trx1 is mainly located in the cytosol, it can migrate to the nucleus upon oxidative stress or be secreted out of the cell [164], while Trx2 represent the vital mitochondrial redox isoform [165]. Both isoforms have a key role in the regulation of cell death, as they interact with and inhibit apoptosis signal regulatory kinase-1 (ASK-1), a kinase belonging to the mitogen-activated protein kinase (MAPK) family capable of promoting apoptotic cell death [166]. Corresponding to the isoforms of mammalian Trx proteins, two different types of TrxR enzyme (TrxR1, TrxR2) exist and are encoded by two distinct genes [167]. TrxR is a homodimeric selenoenzyme with a molecular weight of 55 kDa whose main role is to maintain Trx in its reduced form, in addition to its ability to reduce a substrate, for example ascorbic acid or lipoic acid [168]. Structurally, in addition to catalytic site, TrxR contains a NADPH binding site and a redox active site with a dithiol/disulfide motif [169].

The proposed mechanism of action provides a non-covalent binding between the reduced form of Trx and the oxidized disulfide-containing protein substrate surrounding the Trx active site; subsequently, Trx catalyzes the reduction of disulfides within the oxidized cellular proteins. Finally, oxidized Trx is reduced by TrxR enzyme which consumes/reduces NADPH to $NADP^+$ [170] (Figure 6).

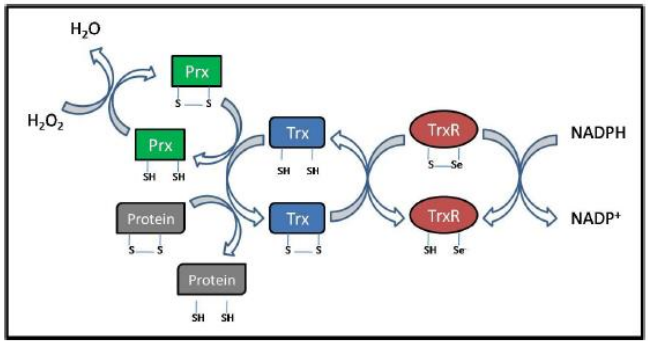

Figure 6. Mechanism of action of the Trx antioxidant mechanism [171]

Moreover, Trx cooperates with peroxiredoxins (Prx) to explain its antioxidant defense function. Prx play a key role in the removal of organic and inorganic peroxides such as H_2O_2 and different alkyl hydroperoxides. The oxidized form of Prx can then be recycled back to its reduced form by Trx [172] (Figure 6).

Since Trx system has a crucial role in the regulation of the balance between antioxidant and oxidative stress it can be associated with NAFLD and tumor progression. Therefore, it is not surprising that dysfunctional or altered expression of Trx is involved in the development of both diseases. Increased Trx1 protein levels are found in many human tumors [164, 173] including breast cancer, in which the overexpression of Trx1 enhances cancer cell growth [174]. Bhatia et al. demonstrated that breast cancers present elevated expression of Trx when compared to normal breast tissue [175]. Moreover, high levels of Trx were associated with poor prognosis and outcome in non-small cell lung carcinoma patients [176] and promoted cancer progression in patients with gastric tumor [177]. Moreover, Trx1 ability to reduce ROS levels confers cell-death resistance to prostate cancer cells, thus promoting tumor progression [178].
Moreover, serum Trx levels distinguish the different stages of NAFLD since patients with NASH show higher levels of Trx than early-stage fatty liver bearing patients [179]. Based on this evidence, targeting the Trx system may provide an innovative therapeutical approach and could improve the NAFLD prognosis.

4.2 Inhibitors of Trx system

Trx system can have bidirectional functions in the development and propagation of the liver disease: at an early stage, its direct antioxidant function is beneficial for preventing normal cell aggressiveness via defending against oxidative stress caused by xenobiotics or carcinogens. However, once healthy cells have initiated malignant transformation, the elevated level of Trx/TrxR may facilitate disease progression and metastasis thus promoting tumor growth, apoptosis resistance, and ultimately therapy resistance [180]. Therefore, since Trx system is usually overexpressed in cancer with respect to non-tumor tissue, there is an increasing interest in developing molecules that target the Trx system, especially the selenoprotein TrxR [181].
A biological inhibitor of the Trx/TrxR mechanism is thioredoxin interacting protein (TXNIP), which binds Trx through the formation of a stable complex, inhibiting a catalytic action of the redox protein [182]. Under normal conditions, TXNIP is mainly located in the nucleus, where it regulates the expression of Trx1, while oxidative stress causes nuclear TXNIP to be transported to the mitochondria where it can inhibit

the action of Trx2 [183]. Overexpression of TXNIP determines significant inactivation of Trx in tumor cells, leading to a block of cell proliferation and an increase of apoptosis susceptibility [183]. In contrast, some tumors, for instance leukemia, showed a significant reduction of TXNIP expression, associated with a high activity of the Trx system [184].

Therefore, therapeutic approaches involve the use of inhibitors of natural or synthetic origin. The principal natural compounds that inhibit Trx system is curcumin, which irreversibly blocks the activity of TrxR causing alkylation of the C-terminal redox active site. Moreover, curcumin decreased NAFLD severity and increased steatosis resolution, in association with a significant decrease in hepatic fibrosis, liver enzymes and total cholesterol in NAFLD patients [185, 186]. Although curcumin is widely used, its effectiveness is still under debate due to its countless targets [187]. Similar inhibition has been observed with myricetin and adenanthin drugs, which induce oxidative stress-mediated cell death of cancer cells [188].

In addition to natural compounds, several synthetic inhibitors of Trx system have been proposed for disease treatment. PX-12 is a potent inhibitor of Trx that alkylates cysteine residues of catalytic center. Moreover, PX-12 is a substrate for TrxR, and thus it acts as a competitive inhibitor to inhibit the reduction of oxidized Trx by TrxR [189]. PX-12 has been tested in the treatment of patients with advance and metastatic cancers (e.g. non-small cell lung cancer, pancreatic, breast, and gastrointestinal cancers), determining a decrease in Trx antioxidant activity and an impairment of its ability to bind to ASK-1, leading to the activation of MAPK [190].

TrxR can be inhibited by compounds that contain metals, for example gold, platinum and silver or Zn [191, 192]. While TrxR strongly binds particularly toxic metals, its substrate Trx is also a heavy metal-binding protein. This probably means that the substrate can help protect the enzyme itself from the inhibition exerted by the metal ion when the total concentration of the latter is substantially lower than the concentration of Trx [193]. Platinum complexes include cis-platinum and carboplatin, which can highly inhibit the activity of TrxR as they show a greater affinity for the selenol group present in the TrxR active center. In addition to interacting with DNA, platinum compounds have been shown to reduce proliferation in breast and ovarian cancers [194], via the disruption of the TrxR system [195]. Moreover, gold compounds have a similar TrxR inhibition mechanism to platinum molecules, and the principal representative of this family is auranofin. *In vitro* studies have shown that auranofin is capable of inhibiting TrxR at nanomolar concentration [196]. Auranofin is approved for rheumatoid arthritis treatment [197] and is currently in clinical trials for different types of cancer [198, 199]. Indeed, treatment with auranofin inhibited the proliferation

of mesothelioma cells and caused an increase in ROS production determining apoptosis of ovarian cancer cells [200]. Moreover, auranofin can disrupt protein homeostasis in HepG2 liver HCC cells and MCF7 breast cancer cells, causing protein degradation and consequently cell death [201]. Finally, auranofin is the only inhibitor tested in NAFLD disease: in NASH model mice fed on a western diet, auranofin reduced liver fibrosis and lipid accumulation [202] in addition to attenuate the inflammatory state and antioxidant markers expression in HFD-fed mice and LX-2 hepatic stellate cell [202, 203]. Therefore, auranofin may have potential as a candidate for NASH treatment.

5. The relevance of sex in the preclinical *in vitro* NAFLD models

Since no pharmacological treatment is currently approved for NAFLD, basic and preclinical research remains essential to improve our understanding of NAFLD pathophysiology and for subsequent therapy development. For instance, *in vitro* models offer the possibility of understanding the mechanisms underlying diseases and studying the effects of therapies at the cellular and molecular level. However, the *in vitro* model used can vary depending on the type of research being carried out and it is unlikely that a single *in vitro* model can recapitulate the *in vivo* complexity of the human liver.

Indeed, a major challenge faced by translational research is related to the small percentage of preclinical findings that are confirmed in the clinic. Consequently, identifying the best models that can help to dissect the molecular and mechanistic insights into liver disease, taking into consideration the sex relevance, is crucial.

The more simplistic *in vitro* models are derived from cell lines cultured in two dimensions; independently of their source, most cell lines can be cultured at a large scale in a cost-efficient manner. However, most of the NAFLD-relevant studies did not specify the sex of the cells, although this aspect would be fundamental to highlight a possible sex-different response to the induction and progression of NAFLD and extrapolate clinically relevant information.

NAFLD is generally induced by the administration of a mixture of unsaturated and saturated free-fatty acid to the culture medium: a commonly used mix is composed by oleic acid added to palmitic or stearic acid in different proportions (accordingly to the different protocols), with the intent to cause a lipid overload into the hepatocytes hence inducing ROS accumulation and subsequent potential lipid peroxides generation [204].

The cellular models that have been used to model NAFLD in the preclinical *in vitro* setting belong to three different classes: immortalized human hepatic cancer cells, primary human hepatocytes (PHH), and stem cells that can be differentiated into hepatocytes (Figure 7).

Human hepatocellular carcinoma cell lines grown as monolayers can be immortalized by genetic engineering or more frequently obtained from male and female human cancers. Hepatic cancer cells commonly used are HepG2 and Huh7, which are derived from male patients, and HepaRG, from a female biopsy: these cells have the advantage of a high proliferative capacity, phenotype stability and reproducibility, ready availability, ease of use and genetic manipulation, low cost of maintenance [205]. However, it is not entirely clear whether they retain a metabolic capacity resembling that of a normal hepatocyte, an aspect that may be key in understanding the lipid metabolic features of NAFLD-induced cells (Figure 7) [206]. Moreover, the use of liver tumor cell lines to study NAFLD progression is not optimal as they may show an important deregulation of metabolic and molecular traits that could be crucial for NAFLD initiation and progression. Of the several hepatic tumor cell lines commercially available [207], the most commonly used is the HepG2 cell line, which originated from the liver biopsy of a 15-year-old Caucasian male. Notably, caution should be used with the HepG2 cell line since (i) has been mistakenly labeled as HCC instead of hepatoblastoma [208] and (ii) displays a weak or absent expression of the cytochrome P450 (CYP) superfamily [209], which is involved in phase 1 xenobiotic oxidation in the liver and also represents a potential source of ROS [210]. HepG2 cells are principally used for drug safety and toxicity assays, molecular target screening [211, 212], and studies related to NAFLD disease and HCC biology [213]. This cell line displays all the main features of a human liver neoplastic transformation (e.g., enhanced protein levels of transferrin and α2-macroglobulin) and is negative for hepatitis virus [214]. Among the male-derived cancer cell lines, Huh7 cells, derived from a well-differentiated HCC in a 57-year-old male, have been rarely used in the context of NAFLD induction [215, 216].

On the other hand, the human hepatoma HepaRG cell line derived from the liver of a European female (age not reported) diagnosed with chronic hepatitis C and macronodular cirrhosis [217, 218] is a female-relevant cellular model. These cells are phenotypically stable thus permitting long-term culture and represent a useful tool in the validation of drugs targeting in 3D organotypic human hepatic steatosis models [218], preclinical drug screening and metabolism assays, and in studies of carcinogenesis and hepatitis B virus (HBV) infection [219, 220].

NAFLD induction using oleic acid administration for a short-term pulse of 16 or 24 hours was reported in different studies using HepG2 [221, 222], with a dose-dependent effect associated with lipid peroxidation and apoptosis [223]. It has been shown that lipid accumulation caused by oleic acid in HepG2 can be significantly reduced by treatment with exendin-4, a GLP-1 receptor agonist [222]. Although no female-derived cell lines were used in the study, a subsequent report demonstrated that exendin-4 is also effective in reducing lipid content and liver inflammation in female mice [224], suggesting that, in this scenario, the observed phenotype is relevant for both sexes. An innovative approach to induce steatosis consists of culturing HepG2 cells in a high-energy mimicking diet using oleic acid and fructose for 24 hours. This condition caused lipid accumulation in HepG2 cells with concomitant alterations in mitochondrial integrity, dynamics, and oxidative phosphorylation, suggesting the dominant role of mitochondria in the first hit of NAFLD progression [225]. Although these data were reported in HepG2 cells, it has been demonstrated that female rats show larger and more functional mitochondria than males pointing to sex hormones as relevant signals in the modulation of mitochondrial biogenesis and function [226, 227]. Estrogen treatment enhanced mitochondrial content and oxidative capacity in the liver of ovariectomized (OVX) rats (i.e., with circulating estrogen levels similar to those of post-menopausal women) and in HepG2 cells, while reducing hepatic lipid accumulation and oxidative stress, suggesting a protective role of estrogens in the liver pathology [228]. Similar results were also obtained in Huh7 cells exposed to oleic acid and palmitic acid in which the estrogen treatment reduced lipid deposition, ROS production, and subsequent lipid peroxidation, a process reverted by the administration of an estrogen receptor antagonist [229].

PHH derived from male and female human donors represent the closest model to study sex dimorphism due to their high similarity with the *in vivo* setting [230]. Although the PHH represent the gold standard short-term human *in vitro* steatotic liver model, they have major limitations as (i) the short propagation time when in culture, (ii) the high phenotypic instability, and (iii) the donor-to-donor variability (Figure 7). NAFLD induction is obtained by exposing PHH to palmitic acid either alone or in combination with oleic acid, a stimulus that leads to lipid accumulation associated with endoplasmic reticulum stress [231] and profibrogenic phenotype [232]. Interestingly, PHH have been cultured in a 3D spheroid system to mimic an *in vivo* human hepatic steatosis [233, 234]: a treatment with free fatty acid and insulin at physiological and pathophysiological concentrations induced a steatotic phenotype and insulin resistance within 21 days [235, 236]. In this context, it would be even more relevant

to specify the sex of the PHH donors as it would further contribute to the investigation of sex differences in the induction and progression of steatosis. However, very few studies were conducted taking this important bias into account. In one of these, PHH obtained from steatotic male and female liver tissues showed no significant difference in the ability to reduce oxidative stress and lipid deposition when exposed to compounds that reduce fat deposition [237].

Finally, in the last decade, the study of NAFLD induction and progression has benefited from the advent of models derived from human embryonic pluripotent stem cells (hESC) and human-induced pluripotent stem cells (hiPSC), which can be differentiated into hepatocyte-like cells (**HLC**). hESC derived from the inner cellular mass of a male or female pre-implanted embryo display pluripotency *in vitro* and *in vivo* and can be differentiated into tissues from all the three germ layers (endoderm, mesoderm, and ectoderm) [238], thus representing an ideal tool to model sex-related phenotypes in liver disease and progression thanks to their high culture stability and reproducibility together with the possibility to be expanded *in vitro* [239, 240]. hiPSC have the advantage that can be obtained from any human somatic cells through the ectopic expression of transcription factors and exhibit unlimited self-renewal ability and ease of accessibility to donor tissues thus enhancing their versatility [241, 242]. Moreover, HLC exhibit morphology, metabolism, and transcriptome profile similar to those of PHH with the advantage of a reduced functionality drift over cell culture passages [243, 244], thus representing an important resource for *in vitro* human liver disease processes investigation. Despite the aforementioned advantages, the use of HLC is limited by ethical restrictions that are different in different countries or by potential issues related to the lack of a standardized differentiation protocol that could lead to an incomplete hepatic differentiation [205] (Figure 7). An important hESC-derived model to study NAFLD progression consists of a 48 hour oleic acid administration to HLC derived from male hESC WA01 cells. This stimulus induces an increase in the intracellular LDs content accompanied by perilipin 2 (PLIN2) and PPAR pathway enhanced expression and activation, respectively. Moreover, Sinton and colleagues proposed a human-relevant model of hepatic steatosis that can be used for high-resolution analysis of metabolic function during NAFLD progression by exposing HLC derived from hESC female to lactate, pyruvate, and octanoate (LPO) [242]. In addition to the canonical macro-vesicular steatosis observed in HLC, LPO stimulation induces the disruption of the electron transport chain activity related to enhanced TCA cycle anaplerosis, with the concomitant compensatory purine nucleotide cycle shunt leading to an overgeneration of fumarate [245]. On these premises, it would be interesting to compare male WA01 and female WA09 cell lines

differentiated in HLC to (i) evaluate potential sex-dependent differences in steatosis etiology and progression and (ii) investigate whether there is a sexual dimorphism related to the oxidant and inflammatory response, thus shedding light on the role of estrogens in this context. Alternatively, a 24 hours oleic acid administration to donor-derived hiPSC differentiated into HLC can be exploited to study NAFLD progression [246].

Using different donors could be relatively straightforward to evaluate the sex- or estrogen-dependent differences in these models. However, HLC derived from hiPSC are mostly used to model the early-stage events of NAFLD. For instance, HLC differentiated from hiPSC derived from 2 male and 2 female donors with liver disease have been exposed to oleic acid for several days, revealing induced lipid accumulation and a distinct steatosis signature for each stage of the liver disease of the donors. This phenotype was paralleled by significant differences in the transcriptome of the four representative models with the highly steatotic cells characterized by low expression of genes associated with gluconeogenesis, phospholipid, and cholesterol biosynthesis together with the concomitant low expression of carnitine palmitoyl transferase 1A (CPT1A), the rate-limiting enzyme responsible for the transport of fatty acid derived acyl-CoA across the mitochondrial membrane, indicating a potential lower capacity of energy generation [247]. Although male and female donors were present in the study, the heterogeneity of the liver disease represented by the models makes it hard to conclude anything meaningful related to sex. Further investigations on additional patients and healthy donor liver specimens are necessary to untangle the contribution of sex hormones-related mechanisms in liver disease progression.

Overall, although many aspects of NAFLD can be recapitulated in vitro, models that take into consideration the genotype, age, and sex of the donors could have a key impact on the analyses of the mechanisms underlying this disease.

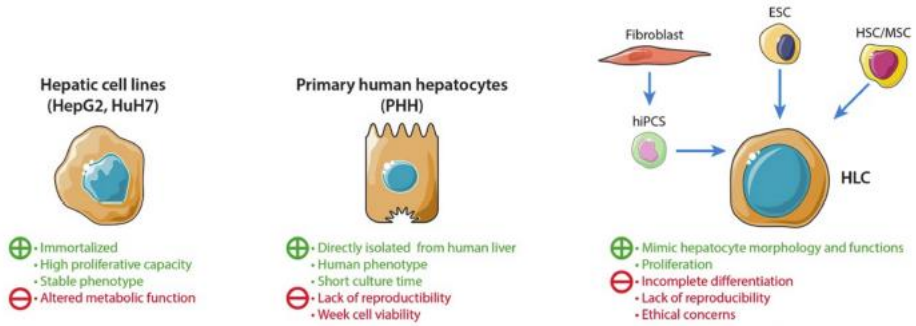

Figure 7. Hepatic cell sources and *in vitro* models of NAFLD [248].

Aim of the thesis

Using a series of *in vitro* experimental models of NAFLD, including human embryonic stem cell-derived hepatocytes and immortalized liver-derived cells, the aim of this thesis is to evaluate the effect of estrogen-signaling in NAFLD initiation and progression with a particular focus on estrogen-dependent antioxidant mechanisms.

Materials and methods

Materials

Common use solutions

- Phosphate buffered saline (PBS): 0.27 g/L di KH_2PO_4, 0.2 g/L KCl, 8.01 g/L NaCl, 1.78 g/L NaH_2PO_4 pH 7.4.
- Lysis buffer: Sample Buffer 1X (SB1X).
- Ripa lysis buffer: (50 mM Tris HCl pH 7.5, 150 mM NaCl, 1% Nonidet P-40, 2 mM EGTA, 1 mM sodium orthovanadate, 100 mM NaF).
- SDS−PAGE 4X Sample Buffer: 40% Glycerol, 240 mM Tris/HCl pH 6.8, 8% SDS, 0.04% bromophenol blue, 5% β-mercaptoethanol.
- SDS-PAGE 1X running buffer: 25 mM Tris, 192 mM glycin, 0.1% (W/V) SDS, pH 8.3.
- Blocking solution: non-fat dry milk 2 %, tween 0.05 % in PBS.
- Washing solution: tween 0.1 % in PBS (T-PBS).
- Protease and phosphatase inhibitors were from Sigma-Aldrich.
- Bicinchoninic acid (BCA) reagent and Bradford reagent for protein dosage were from Sigma-Aldrich and Biorad, respectively.
- Reagents for RNA extraction, cDNA synthesis, and RT-PCR were from Qiagen, Applied Biosystem, and Biorad.

Drugs, compounds, and reagents

- 17β-estradiol (E2, Cat n° E2758), dissolved in 100% ethanol at 1 μM, stored at -20°C, purchased from Sigma.
- Activin A (AA, Cat n° 120-14E), used at a concentration of 100 ng/ml, kept at -20°C; purchased from PeproTech.
- Auranofin (AU, Cat n° A6733), purchased from Sigma-Aldrich.
- β-Mercaptoethanol (Cat n° 31350) used at a concentration of 0.1 mM, maintained at +4°C, purchased from ThermoFisher.
- B27 supplement (Cat n° 17504), purchased from ThermoFisher.
- 4,4-difluoro-1,3,5,7,8-pentamethyl-4-bora-3a,4a-diazas-indacene ($BODIPY^{493/503}$, Cat n° D3922), stored at -20°C, purchased from ThermoFisher.
- Bovin Serum Albumin (BSA, Cat n° A9418) purchased from Sigma-Aldrich.
- CellROX (Cat n° C10444) purchased from ThermoFisher.
- Dexamethasone (Cat n° A13449) purchased from ThermoFisher.
- Dimethyl sulfoxide (DMSO, Cat n° D2650) purchased from Sigma-Aldrich.

- Dulbecco's Modified Eagle Medium (DMEM, Cat n° 11965092) high glucose purchased from ThermoFisher.
- DMEM:F12 (Cat n° 11330032) purchased from ThermoFisher.
- Insulin-Transferrin-Selenium (Cat n°41400045) purchased from ThermoFisher.
- Gentle cell dissociation reagent (Cat n° 07174) purchased from Stem Cell Technologies.
- GlutaMax (Cat n° 35050061) purchased from ThermoFisher.
- Hepatocyte Growth Factor (HGF, Cat n° 100-39), used at a concentration of 10 ng/ml, purchased from PeproTech.
- HepatoZYME medium (Cat n° 17705) purchased from ThermoFisher.
- Hydrocortisone 21-hemisuccinate sodium salt (Cat n° H4881), used at a concentration of 10 µM, purchased from Sigma-Aldrich.
- L-15 medium (Cat n° L1518) purchased from Sigma.
- Knockout DMEM medium (KO-DMEM, Cat n° 10829) purchased from ThermoFisher.
- Knockout Serum Replacement (KO-SR, Cat n° 10828), purchased from ThermoFisher.
- mTeSR1 and supplement (Cat. n° 05850) purchased from Stem Cell Technologies.
- mFeSR1 (Cat n° 05855) purchased from Stem Cell Technologies.
- MitoSOX (Cat n° M36008) purchased from ThermoFisher.
- Non-Essential Amino Acids Solution (NEEA, Cat n° 11140) purchased from ThermoFisher.
- Octanoic Acid (Cat n° C2875) purchased from Sigma-Aldrich.
- Oncostatin M (OSM, Cat n° 300-10), used at a concentration of 20 ng/ml, purchased from PeproTech.
- Penicillin-streptomycin (Cat n° 15140) purchased from ThermoFisher.
- Recombinant human laminin 521 (LMN-521, Cat n° LN521), kept at -80°C, purchased from BioLamina.
- Rho-associated kinase inhibitor (ROCKi, Cat n° 72302) Y27632 kept at -20°C; purchased from StemCell Technologies.
- RPMI 1640 medium (Cat n° 21875) purchased from ThermoFisher.
- Sodium-L-lactate (Cat n° L7022) purchased from Sigma-Aldrich.
- Sodium pyruvate (Cat n° P5280) purchased from Sigma-Aldrich.

- Wingless-Type MMTV Integration Site Family, Member 3 A (wnt3a, Cat n° 1324-WN-500/CF), used at a concentration of 50 ng/ml, kept at -20°C; purchased from PeproTech.

Antibody

Antibody	Dilution	Application	Source	Use	Manufacturer
HNF4α	1:1000	WB	Rabbit	O/n 4°C	Cell Signalling (Cat n° 3113)
E-cadherin	1:1000	WB	Rabbit	O/n 4°C	Cell Signalling (Cat n° 24E10)
TRX2	1:500	WB	Mouse	O/n 4°C	Santa Cruz (Cat n° sc-133201)
ERα	1:1000	WB	Rabbit	O/n 4°C	Abcam (Cat n° ab16660)
Hsp90	1:1000	WB	Mouse	O/n 4°C	Santa Cruz (Cat n° sc-69703)
Histone H_3	1:1000	WB	Mouse	O/n 4°C	Cell Signalling (Cat n° 9715)
β-Actin	1:1000	WB	Mouse	O/n 4°C	Cell Signalling (Cat n° 8H10D10)

Methods

Cell lines and general culture conditions

Male and female human embryonic stem cells (hESCs) lines **H1/WA01** and **H9/WA09**, respectively, were purchased from WiCell. These stem cells grow on an LMN-521 coating at a concentration of 5 µg/mL in mTeSR1 plus 5X supplement medium in the cell colonies form.

When the cells reach 75%-80% confluence, the medium is aspirated, a PBS wash is performed, and the cells are incubated for approximately 5 minutes with 1 mL of gentle cell dissociation reagent to promote their detachment from the LMN-521 coating. After about 5 minutes, the gentle cell dissociation reagent is aspirated, the cells are resuspended with the medium and then transferred to the desired concentration in the new maintenance medium. At the time of differentiation into hepatocytes, however, the stem cells are plated onto the LMN-521 coating as a single cell by adding

ROCKi inhibitor Y27632 to the medium. This inhibitor is used to improve the adhesion and survival of stem cells in single-cell suspensions.

AML12 and HepG2 cell lines were purchased from American Type Culture Collection (ATCC): AML12 cells are hepatocytes isolated from the normal liver of a male mouse and growth in DMEM:F12 (1:1) supplemented with 10% fetal bovine serum (FBS), 10 µg/ml insulin-5.5 µg/ml transferrin-5 ng/ml selenium, and 40 ng/ml dexamethasone; whereas, HepG2 is a human hepatocellular carcinoma cell lines maintained in DMEM high glucose medium supplemented with 10% FBS, 2 mM glutamax, and 1% penicillin/streptomycin.

For cell passaging, growth medium was removed, and the cells were washed with PBS and incubated with a covering volume of trypsin for 1-2 minutes. When cells were detached, medium was added to neutralize trypsin's effect and cells were seeded into a new flask.

Long-term cell frozen storage

Cells were detached using trypsin, resuspended into their cell culture medium, and pelleted by centrifugation at 1.000 rpm (rotation per minute) for 5 minutes. Then, pellet was resuspended in 1 mL of cell freezing medium (90% FBS and 10% DMSO for HepG2 and AML12, mFeSR1 for hESCs) and cells transferred into specific freezing vials, stored in polystyrene insulated boxes at -80°C for at least 48 hours and subsequently in liquid nitrogen for long time. For the thawing procedure, cells were moved into a new flask and resuspended with fresh cell culture medium. The following day, medium was replaced to completely remove DMSO.

Differentiation of hESCs in hepatocyte-like cells

The differentiation protocol of hESCs into hepatocyte-like cells (HLCs) lasts 18 days, during which the cells progress from an embryonic stage to the formation of mature hepatocytes.

hESCs are plated at a concentration of 400,000 cells per well to start differentiation the next day with a 40% confluence. To ensure efficient differentiation, hESC must be small and evenly spaced (Figura 8).

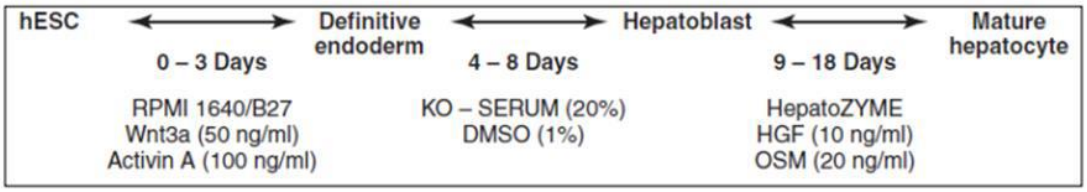

Figure 8. Outline of the differentiation process and planned treatments.

Phases of the differentiation process into HLCs:

1st phase: The first phase lasts three days during which we obtain the endoderm cells from the stem cells. We used RPMI 1640 medium supplemented with B27 supplement (50X) and endodermal growth factors such as wnt3a (50 ng/mL) and AA (100 ng/mL). At the end of this first phase, we begin to observe the first morphological changes of the cells.

2nd phase: From day 4 to day 8, we obtain the precursor cells of hepatocytes, called hepatoblasts. These cells growth in KO-DMEM medium supplemented with 20% KO-SR, 1% penicillin/streptomycin, 1% DMSO, 1% NEEA, 0.5% glutamax and 0.2% β-mercaptoethanol. At the end of this phase, hepatoblasts showed the classic "tile" morphology of hepatocytes.

3rd phase: From day 9 to day 18, we obtain HLCs from the hepatoblasts. We used HepatoZYME medium supplemented with 1% glutamax, 1% streptomycin penicillin, 20 ng/mL of HGF, 10 ng/mL of OSM and 10 µM hydrocortisone 21-hemisuccinate sodium salt (Figure 9).

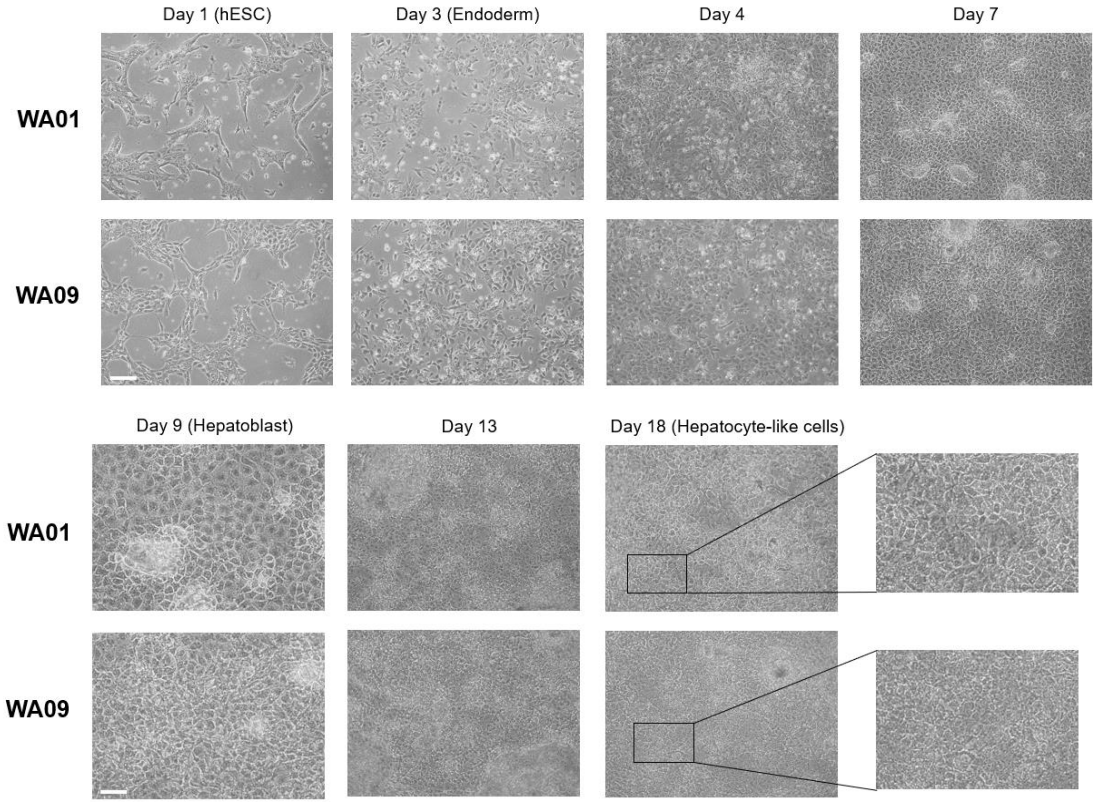

Figure 9. Phases of the differentiation process of hESCs into HLCs.

Protein analysis

Protein extraction: cells were washed twice in cold PBS and then lysed with SB1X supplemented with protease and phosphatase inhibitors (1/100). Protein lysates were collected, kept in ice, and centrifuged at 12.000 rpm for 10 minutes. After centrifugation, the supernatant was collected, and total proteins were quantified with either BCA protein assay or Bradford assay.

Protein quantification: The BCA protein assay is based on the notion that proteins can reduce Cu^{+2} to Cu^{+1} in an alkaline solution containing BCA resulting in a purple color formation. The absorbance of the BCA/copper complex at 562 nm is directly proportional to the protein concentration. To prepare BCA solution, we combined 50 parts of A solution with 1 part of B solution. In cuvettes for spectrophotometer, we added 45 uL of water (50 uL for the blank), 5 uL of each protein lysate sample, and 950 uL of BCA solution. After 30 minutes of incubation at 37°C, all the samples and the blank were read by the spectrophotometer at a wavelength of 562 nm.
To generate the standard curve, we used BSA diluting BSA 2 mg/mL concentrated in dH2O to obtain BSA concentrations from 2 µg/mL to 15 µg/mL. Thus, from the values obtained from the standard curve, it is possible to create a curve of the absorbance in function of the concentration; consequently, interpolating absorbance values to the standard curve, it is possible to calculate the final protein concentration of the samples of interest. Correlation between absorbance and concentration is expressed by Lambert-Beer law: $A=\varepsilon dc$, where ε represents the molar extinction coefficient, d represents the path length, and c the sample concentration.

SDS-PAGE: it is a technique used for protein separation thanks to their ability to move within an electric current, which is a function of the length of their polypeptide chains or of their molecular weight. This is achieved by adding SDS detergent to remove secondary and tertiary protein structures and to maintain the proteins as polypeptide chains. SDS-PAGE samples were boiled for 5 minutes in SB 4x plus β-mercaptoethanol, which leads to disulphuric bond reduction and destabilization of protein tertiary structure. The gels used were precast SDS-PAGE gels (Biorad), with a range of acrylamide concentration from 4% to 20%, required to better stratify the samples before entering the separating gel. 20-40 µg of total proteins were loaded into the wells of the stacking gel and an electric field was applied across the gel, allowing the negatively charged proteins to migrate across the gel towards the positive electrode (anode). Protein relative molecular mass was evaluated by comparison with

protein ladder standard molecular weights, separated into the same gel. Running was performed at 100-150 V for almost 1 hour.

Western blotting

After running, protein samples were transferred from the gel to a nitrocellulose membrane (blotting) by Trans-Blot Turbo Transfer Pack (Biorad) to make the proteins accessible for the antibody detection. The proteins embedded into the gel are transferred to the membrane maintaining the organization that they have within the gel. Protein transfer was carried out at 25 V and 2.5 A for 7 minutes (for proteins with low molecular weight). After blotting, the membrane was incubated for 1 hour in the blocking solution (non-fat dry milk 2%, tween 0.05% in PBS) at room temperature and then overnight in slow agitation at 4°C in a blocking solution with the specific primary antibody. The following day, the membrane was washed three times with a solution of T-PBS and then incubated with the horseradish peroxidase (HRP)-conjugated secondary antibody for 1 hour at room temperature and finally washed again for three times with T-PBS. In the chemiluminescence reaction, HRP catalyzes the oxidation of luminol into a reagent which emits light when it decays. Since the HRP is complexed with the secondary antibody specific for the protein of interest on the membrane, amount and location of the emission light are directly correlated with those of the protein of interest. Chemiluminescent protein revelation was carried out with ECL Western Blotting reagents (Biorad) at the Amersham Imager 600. Exposure was repeated varying the time as needed for the optimal detection.
The antibodies used for protein detection are summarized in table.

RNA manipulation

Total RNA was extracted from cultured cells, grown as monolayer, using RNeasy Mini Kit (Qiagen). RNA concentration and quality of the samples were determined by measuring the UV absorbance at 260 nm and 280 nm on Nanodrop 1000 (Thermo Scientific), and 500 ng of total RNA were reverse transcribed to cDNA using QuantiTect cDNA reverse transcription kit (Qiagen), according to manufacturer's instructions.
Moreover, total RNA, including small RNA, was extracted using miRNeasy Mini Kit (Qiagen), quantified, and 10 ng were reverse transcribed using Taqman MicroRNA Reverse Transcription Kit (Applied Biosystems) for miRNA analysis, according to manufacturer's instructions.

Quantitative Real-Time Polymerase Chain Reaction

qRT-PCR is a method by which the amount of the PCR product can be determined in real-time and is useful for investigating gene expression using a fluorescent reporter whose signal strength is directly proportional to the number of amplified DNA molecules. qRT-PCR was done the CFX96 Touch Real-Time PCR Detection System (Biorad), employing Taqman gene/miRNA assays (Applied Biosystems).

The probes used in the first part of the work are: Albumin (Hs00609411_m1), HNF4α (Hs00230853_m1), Txn2 (Hs00429399_g1), PLIN2 (Hs00605340_m1 and Mm00475794_m1), ACLY (Hs00982738_m1), GDF15 (Hs00171132_m1), SLC34A2 (Hs00197519_m1), NRF2 (Hs00975961_g1), NQO1 (Hs01045993_g1), TBP (Hs00427620_m1), ACTB (Mm02619580_g1) for mRNA analysis. For miRNA assay, the probes used is endogenous controls RNU48 (ID:001006). The relative quantity was determined using $\Delta\Delta^{Ct}$, according to the manufacturer's instructions (Applied Biosystems).

Confocal analysis

Cell lines are plated at a concentration of 10,000 cells per well, in a Nunc™ Lab-Tek™ Chamber Slide System (ThermoFisher). Once the cells have been plated and NAFLD has been induced, they can be labeled with different fluorescent probes: for example, the CellRox probe emits green fluorescence with excitation/emission maxima of 485/520nm and is used to the measurement of cytoplasmic and nuclear ROS production, with an incubation lasting 30 minutes. Another probe for oxidative stress detection is MitoSox, which emits red fluorescence with 488/510 nm and is used to the measurement of mitochondrial ROS production.

To evaluate the accumulation of intracellular lipids, the cells are marked for 15 minutes with the BODIPY$^{493/503}$ nm probe, a lipophilic dye capable of penetrating the cell, binding to the lipid accumulations and emitting fluorescence.

Once the incubation with the probes has been completed and the medium has been aspirated, the cells are fixed using a 4% formaldehyde solution for 10 minutes. Subsequently, the formaldehyde is aspirated, and three washes are performed in PBS. To stain the nuclei, the cells are then incubated for 10 minutes with the DAPI$^{358/461}$ nm dye (diluted 1:1000 in PBS) and subsequently washed an additional 3 times in PBS. Finally, each well is viewed under a confocal microscope.

ROS detection

To evaluate intracellular ROS production, cells are initially plated at a concentration of 70,000 cells, per well, in 12-well culture dishes. Once NAFLD has been induced, the cells can be incubated with CellRox probe for 30 minutes.

Subsequently, the cells are lysed in RIPA Buffer, using scrapers and the fluorescence is evaluated using the *Synergy H1 Hybrid Multi-Mode Reader* (Biotek) plate reader. Normalization of the obtained data can be performed on protein content or cell count, depending on the cell line and media.

Flow cytometric analysis

Cell lines are plated at a concentration of 70,000 cells, per well, in a 12-well culture dishes and incubated with different fluorescent probes (CellRox and BODIPY$^{493/503}$). Once the incubation time with the probe has concluded, the cells are incubated for a few minutes in 500 µL of Trypsin. Subsequently, 1 mL of medium is added, and the cells are resuspended to facilitate their detachment from the well. The total volume is then transferred into specific tubes for the flow cytometer, which will then be centrifuged for 5 minutes at 1200 rpm. Subsequently, the supernatant is discarded while the pellet is resuspended in 400 µL of a solution composed of PBS+1% FBS. Once this procedure is completed, the samples are analysed by flow cytometry.

In silico analysis for Trx2 expression

Transcriptomic raw data are available at the National Center for Biotechnology Information GEO repository (accession number GSE163211). Gene expression data were analyzed using *R*. The statistical test performed is Wilcox test, $p < 0.05$. Statistical significance was defined as: $p<0.05$.

```
library(ggplot2)
library(ggpubr)
library(readxl)
Table<-read_xlsx(path="Cartel1.xlsx", col_names = T)
Table<-as.data.frame(Table[ , colnames(Table)!="...4"])
head(Table, n=3)

Table$Age<-gsub("age: ","",Table$Age)
Table$Age <- as.numeric(Table$Age)
Table$Sex<-gsub("Sex: ","",Table$Sex)
Table$Stage<-gsub("nafld stage: ","",Table$Stage)
Table_FM <- Table[Table$Sex=="Female",]

colnames(Table_FM)<-gsub(" ","_",colnames(Table_FM))
Table_FM$TXN2_value<-as.numeric(Table_FM$TXN2_value)
Table_FM$Stage <- factor(Table_FM$Stage, levels =
c("Normal","Steatosis","NASH_F0","NASH_F1_F4"))
```

```
# plotting
ggplot(aes(x=Stage, y=TXN2_value, fill=Sex), data=Table_FM)
  geom_boxplot() +
  theme_classic() +
  theme(axis.text.x = element_text(angle=20, size=9, hjust=1, vjust=1) ) +
  labs(fill="", y= "TXN2 expression", x="")
ggsave(file="All stage_all female.png", dpi=300, width = 5, height = 4)

## statistical analysis
Table_FM_2<-Table_FM[Table_FM$Stage %in% c("Normal","Steatosis") , ]
wilcox.test(TXN2_value ~ Stage , Table_FM_2, paired=F ) # Mann W
#p-value = 0.7657
Table_FM_3<-Table_FM[Table_FM$Stage %in% c("Normal","NASH_F0") , ]
wilcox.test(TXN2_value ~ Stage , Table_FM_3, paired=F ) # Mann W
#p-value = 0.006299
Table_FM_4<-Table_FM[Table_FM$Stage %in% c("Normal","NASH_F1_F4") , ]
wilcox.test(TXN2_value ~ Stage , Table_FM_4, paired=F ) # Mann W
#p-value = 4.29e-05
Table_FM_5<-Table_FM[Table_FM$Stage %in% c("Steatosis","NASH_F0") , ]
wilcox.test(TXN2_value ~ Stage , Table_FM_5, paired=F ) # Mann W
#p-value = 0.004775
Table_FM_6<-Table_FM[Table_FM$Stage %in% c("Steatosis","NASH_F1_F4") , ]
wilcox.test(TXN2_value ~ Stage , Table_FM_6, paired=F ) # Mann W
#p-value = 3.028e-05
Table_FM_7<-Table_FM[Table_FM$Stage %in% c("NASH_F0","NASH_F1_F4") , ]
wilcox.test(TXN2_value ~ Stage , Table_FM_7, paired=F ) # Mann W
#p-value = 0.07811

#########################################################################
library(ggplot2)
library(readxl)
Table<-read_xlsx(path="Cartel1.xlsx", col_names = T)
Table<-as.data.frame(Table[ , colnames(Table)!="...4"])
head(Table, n=3)

Table$Age<-gsub("age: ","",Table$Age)
Table$Age <- as.numeric(Table$Age) # coercizzo in numerico
Table$Sex<-gsub("Sex: ","",Table$Sex)
Table$Stage<-gsub("nafld stage: ","",Table$Stage)

Table_FM <- Table[Table$Sex=="Female",]
Table_F_OLDER <- Table_FM %>% filter(Age >= 50)
colnames(Table_F_OLDER)<-gsub(" ","_",colnames(Table_F_OLDER))
Table_F_OLDER$TXN2_value<-as.numeric(Table_F_OLDER$TXN2_value)
Table_F_OLDER$Stage <- factor(Table_F_OLDER$Stage, levels = c("Normal",
"Steatosis","NASH_F0","NASH_F1_F4"))

# plotting
ggplot(aes(x=Stage, y=TXN2_value, fill=Sex), data=Table_F_OLDER)
  geom_boxplot() +
  theme_classic() +
  theme(axis.text.x = element_text(angle=20, size=9, hjust=1, vjust=1) ) +
  labs(fill="", y= "TXN2 expression", x="")
ggsave(file="All stage_OLDER female.png", dpi=300, width = 5, height = 4)
```

```
## statistical analysis
Table_FM_2<-Table_F_OLDER[Table_F_OLDER$Stage %in% c("Normal","Steatosis") , ]
wilcox.test(TXN2_value ~ Stage , Table_FM_2, paired=F ) # Mann W
# p-value = 0.3861
Table_FM_3<-Table_F_OLDER[Table_F_OLDER$Stage %in% c("Normal","NASH_F0") , ]
wilcox.test(TXN2_value ~ Stage , Table_FM_3, paired=F ) # Mann W
#p-value = 0.02047
Table_FM_4<-Table_F_OLDER[Table_F_OLDER$Stage %in% c("Normal","NASH_F1_F4") , ]
wilcox.test(TXN2_value ~ Stage , Table_FM_4, paired=F ) # Mann W
#p-value = 2.149e-05
Table_FM_5<-Table_F_OLDER[Table_F_OLDER$Stage %in% c("Steatosis","NASH_F0") , ]
wilcox.test(TXN2_value ~ Stage , Table_FM_5, paired=F ) # Mann W
#p-value = 0.2709
Table_FM_6<-Table_F_OLDER[Table_F_OLDER$Stage %in% c("Steatosis","NASH_F1_F4")
, ]
wilcox.test(TXN2_value ~ Stage , Table_FM_6, paired=F ) # Mann W
#p-value = 0.002898
Table_FM_7<-Table_F_OLDER[Table_F_OLDER$Stage %in% c("NASH_F0","NASH_F1_F4") ,
]
wilcox.test(TXN2_value ~ Stage , Table_FM_7, paired=F ) # Mann W
#p-value = 0.03789

#############################################################################
Table_FM <- Table[Table$Sex=="Female",]
Table_F_YOUNGER <- Table_FM %>% filter(Age <= 50)
colnames(Table_F_YOUNGER)<-gsub(" ","_",colnames(Table_F_YOUNGER))

Table_F_YOUNGER$TXN2_value<-as.numeric(Table_F_YOUNGER$TXN2_value)
Table_F_YOUNGER$Stage <- factor(Table_F_YOUNGER$Stage, levels = c("Normal",
"Steatosis","NASH_F0","NASH_F1_F4"))

# plotting
ggplot(aes(x=Stage, y=TXN2_value, fill=Sex), data=Table_F_YOUNGER)
  geom_boxplot() +
  theme_classic() +
  theme(axis.text.x = element_text(angle=20, size=9, hjust=1, vjust=1) ) +
  labs(fill="", y= "TXN2 expression", x="")
ggsave(file="All stage_YOUNGER female.png", dpi=300, width = 5, height = 4)

## statistical analysis
Table_FM_2<-Table_F_YOUNGER[Table_F_YOUNGER$Stage %in% c("Normal","Steatosis")
, ]
wilcox.test(TXN2_value ~ Stage , Table_FM_2, paired=F ) # Mann W
# p-value = 0.5028
Table_FM_3<-Table_F_YOUNGER[Table_F_YOUNGER$Stage %in% c("Normal","NASH_F0") ,
]
wilcox.test(TXN2_value ~ Stage , Table_FM_3, paired=F ) # Mann W
#p-value = 0.05077
Table_FM_4<-Table_F_YOUNGER[Table_F_YOUNGER$Stage %in% c("Normal","NASH_F1_F4")
, ]
wilcox.test(TXN2_value ~ Stage , Table_FM_4, paired=F ) # Mann W
#p-value = 0.007545
Table_FM_5<-Table_F_YOUNGER[Table_F_YOUNGER$Stage %in% c("Steatosis","NASH_F0")
, ]
wilcox.test(TXN2_value ~ Stage , Table_FM_5, paired=F ) # Mann W
#p-value = 0.004675
Table_FM_6<-Table_F_YOUNGER[Table_F_YOUNGER$Stage %in%
c("Steatosis","NASH_F1_F4") , ]
```

```
wilcox.test(TXN2_value ~ Stage , Table_FM_6, paired=F ) # Mann W
#p-value = 0.000526
Table_FM_7<-Table_F_YOUNGER[Table_F_YOUNGER$Stage %in%
c("NASH_F0","NASH_F1_F4") , ]
wilcox.test(TXN2_value ~ Stage , Table_FM_7, paired=F ) # Mann W
#p-value = 0.4082
```

Statistical analysis

All experiments were conducted at least 3 times independently Statistical analysis of the data was performed using GraphPad Prism Software. Unless stated otherwise, comparisons between 2 groups were made using the two-tailed, unpaired Student's t-test. Comparisons between multiple groups were made using one-way or two-way analysis of variance (ANOVA). Bonferroni and Dunnett post-testing analysis with a confidence interval of 95% was used for individual comparisons as reported in figure legends. Statistical significance was defined as: * $p<0.05$; **$p<0.01$; ***$p<0.001$; ****$p<0.0001$; when differences were not statistically significant, or the comparison not biologically relevant, either no indications were reported in the figures or indicated with ns.

RESULTS

Phenotypic and functional characterization of HLCs derived from hESC

Male WA01 and female WA09 hESC were differentiated into HLCs using a previously published protocol [249]. The success of the differentiation process was controlled by monitoring mRNA and protein levels of an established hepatic markers.

In addition to the acquisition of a classic cobblestone-like hepatic morphology (**Figure 9**), HLCs derived from both hESC cell lines showed an increase of both protein and mRNA levels of the hepatic markers Albumin and Hepatocyte Nuclear Factor-4-alpha (HNF4α) (**Figure 10A,B**). Moreover, we also observed a higher protein level of E-Cadherin (E-Cad), an important molecule responsible for the assembly and functionality of adherent junctions, which is typical of differentiated hepatocyte (**Figure 10B**). This approach allowed us to recapitulate an interesting differentiation protocol using sex-matched hESC and thus generating a highly reproducible and functional hepatocyte model, useful to study hepatic disease in a sex-relevant setting.

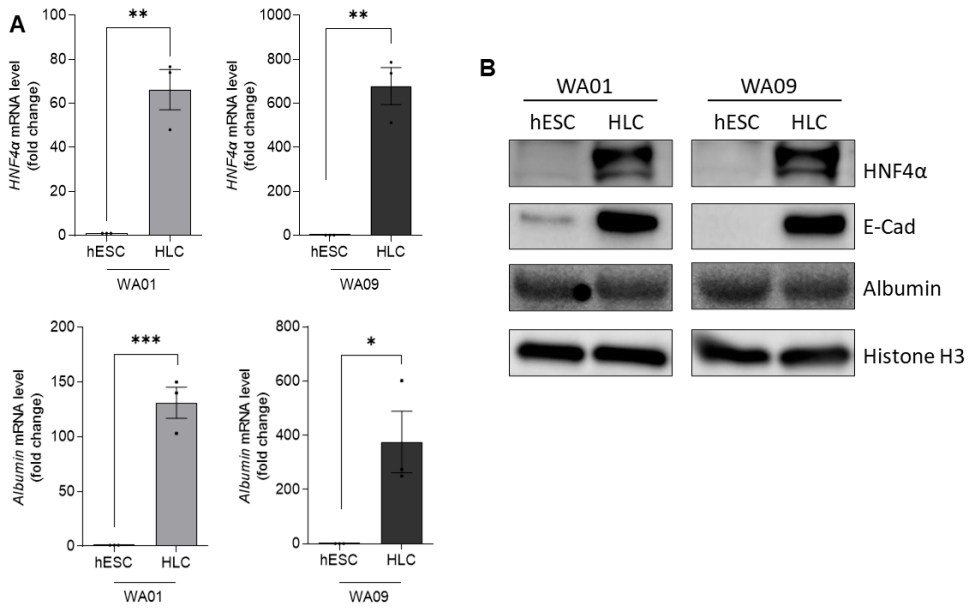

Figure 10. Phenotypic and functional characterization of HLCs derived from hESC. (**A**) HLCs derived from male WA01 and female WA09 hESC were subjected to qRT-PCR analysis. Relative expression is shown using the hESC as comparator. Data represent means ± SEM. *p < 0.05; **p < 0.01; ***p < 0.001. Each dot represents a biological replicate. (**B**) Total protein lysates from male WA01 and female WA09 hESC and HLCs were subjected to western blot analysis with the antibody indicated. The Histone H_3 is used as protein loading control normalizer.

Steatosis was induced in HLCs and immortalized cells by treatment with sodium L-lactate, sodium pyruvate, and octanoic acid

To mimic an *in vitro* model of steatosis, in addition to HLCs, we used two other immortalized liver cell lines that have been extensively used to study NAFLD initiation and progression: AML12, hepatocytes isolated from a normal murine liver [250], and HepG2, a cell line that was erroneously identified as hepatocellular carcinoma rather than hepatoblastoma [208].

The steatotic phenotype (also known as NAFL-induced phenotype) was induced by treating each cell model used (HLCs, AML12 or HepG2) with a cocktail of compounds composed of sodium L-lactate (L), sodium pyruvate (P), and octanoic acid (O), hereafter referred as LPO, for 48 hours (**Figure 11A**) [251]. Following LPO treatment, HLCs subjected to NAFL significantly reduced mRNA (**Figure 11B**) and protein (**Figure 11C**) expression of the aforementioned established hepatic markers, a sign of a clear dysfunction of the hepatocytes.

Steatosis consists in the intracellular accumulation of lipids within the cytoplasm of the hepatocyte, in the form of lipid droplets (LDs), dynamic and multifunctional organelles involved in energy metabolism, signaling, and inflammatory mediator production [252]. To determine whether steatosis was induced in HLCs and immortalized cells following LPO treatment, we performed confocal and FACS analyses using the fluorescent neutral lipid dye BODIPY$^{493/503}$ which is retained in LDs. Confocal analysis and subsequent quantification showed that steatotic WA01 and WA09 are significantly enriched in LDs content (**Figure 11D**). Moreover, also in AML12 and HepG2 cell lines, LPO treatment significantly increased LDs, as observed by confocal and FACS analyses, when compared to untreated conditions (**Figure 11E**). In parallel, LPO-exposed WA01, WA09, AML12 and HepG2 cells express higher mRNA levels of the members of the Perilipin (PLIN) family proteins, namely PLIN2 (**Figure 11F**), whose expression correlates with LDs content in hepatocytes of HFD-fed mice [253].

Since oxidative stress contributes to the NAFLD progression, we analyzed reactive oxygen species (ROS) production in healthy and LPO-induced cells. Indeed, mitochondrial and cytoplasmatic ROS levels, detected by MitoSOX and CellRox fluorescent probe, respectively, were increased in steatotic HLCs with respect to healthy HLCs (**Figure 11G**). Moreover, evaluation of oxidative stress in AML12 and HepG2 cell lines upon LPO administration showed enhanced CellRox levels, either detected by confocal or fluorometric analyses (**Figure 11H,I**).

Altogether these data showed that steatotic hepatic model based on LPO induction in HLCs, AML12 and HepG2 cells is a robust approach that can be used for studying NAFLD disease.

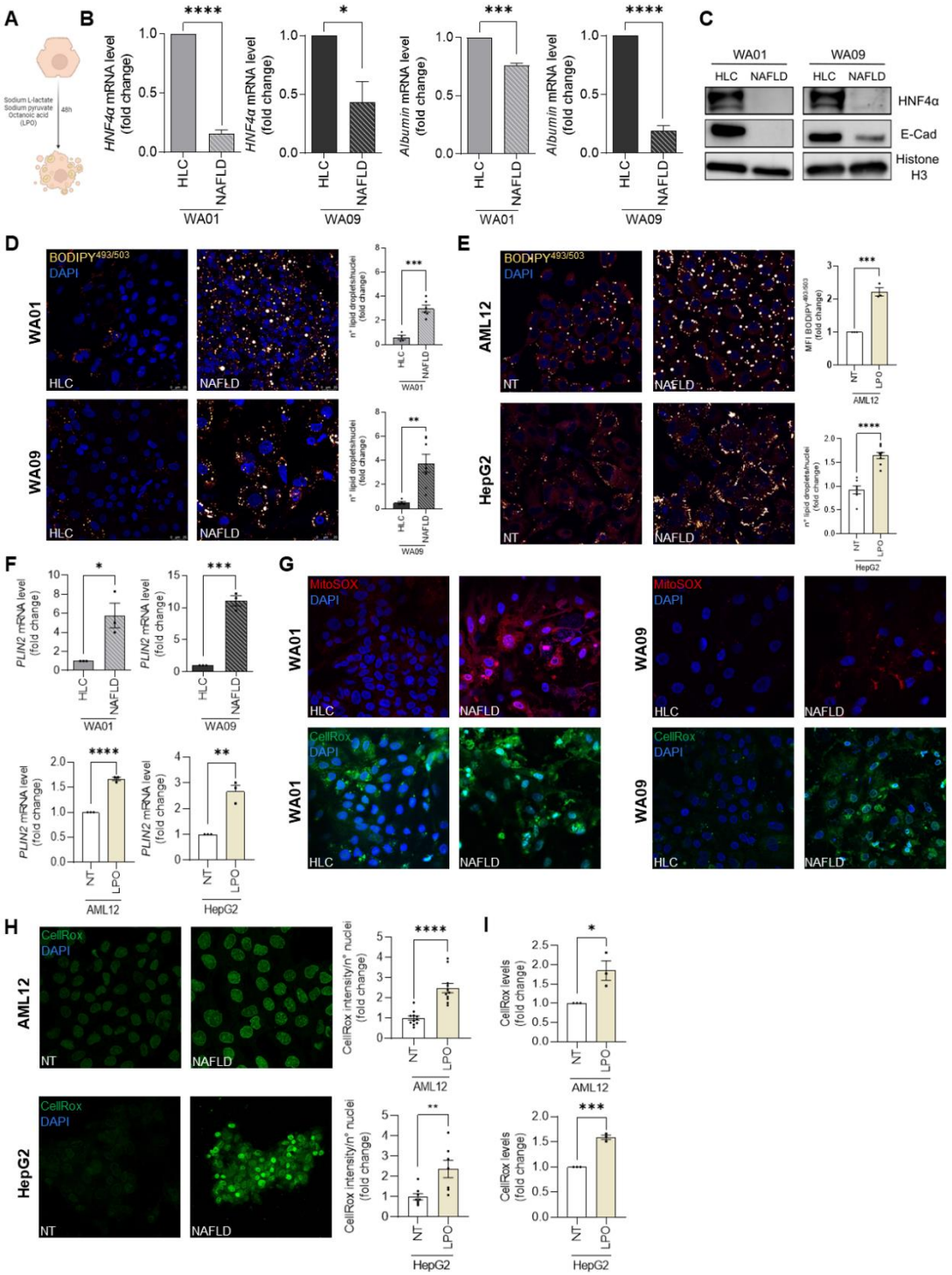

Figure 11. Steatosis was induced in HLCs and immortalized cells by treatment with sodium L-lactate, sodium pyruvate, and octanoic acid. (**A**) Schematic representation of NAFL induction in hepatic cell models: treatment with 10 mM sodium L-lactate (L), 1 mM sodium pyruvate (P), and 2 mM octanoic acid (O) (LPO) for 48 hours. (**B-C**) HLCs and LPO-exposed WA01 and WA09 cells were subjected to qRT-PCR (**B**) and western blotting (**C**) analyses using the assays described in the figure. Data represent means ± SEM. Student's t test *p < 0.05; **p < 0.01; ***p < 0.001. Each dot represents a biological replicate. (**D-E**) Basal

and LPO-exposed (**D**) WA01, WA09, (**E**) AML12 and HepG2 cells were subjected to confocal and FACS analyses. Representative pictures of BODIPY$^{493/503}$ stained cells are shown (orange/yellow: LDs; blue: DAPI, nuclei). Quantification of BODIPY spots/cell was reported. Scale bar, 10 μm. The mean fluorescence intensity (MFI) of the populations positive for BODIPY$^{493/503}$ recovered by FACS analysis was reported. (**F**) Basal and LPO-exposed WA01, WA09, AML12 and HepG2 cells were subjected to qRT-PCR analysis. Data represent means ± SEM. Student's t test *p < 0.05; **p < 0.01; ***p < 0.001. Each dot represents a biological replicate. (**G**) Basal and LPO-exposed WA01, WA09 cells were subjected to confocal analysis. Representative pictures of MitoSOX and CellRox stained cells are shown (Red: MitoSOX; Green: CellRox; blue: DAPI, nuclei). (**H-I**) AML12 and HepG2 cells were treated with LPO for 48 hours and subjected to confocal and fluorescent analyses. (**H**) Representative pictures of CellRox stained cells are shown (Green: CellRox; blue: DAPI, nuclei). Quantification of CellRox was reported. Scale bar, 10 μm. (**I**) ROS levels were measured using the fluorescent probe CellRox in AML12 and HepG2 cells treated with LPO. Untreated cells were used as comparator. Data represent means ± SEM. Student's t test *p < 0.05; ***p < 0.001. Each dot represents a biological replicate.

Estrogens reduce LDs accumulation and oxidative stress in steatotic cells

The lower incidence of NAFLD in pre-menopausal women when compared to post-menopausal and men prompted us to postulate that sex hormones, i.e., estrogens, could have a protective role in disease onset and/or progression.

Initially, we evaluated whether 17β-estradiol (E2), the major female sex hormone, could induce E2-dependent transcriptional changes in LPO-treated cells. Indeed, treatment with 1 nM E2 for 48 hours increased mRNA expression of estrogen-related liver-specific genes [254], such as growth differentiation factor 15 (GDF15) and solute carrier family 34 member 2 (SLC34A2), in both steatotic HLCs derived from male WA01 and female WA09 cells (**Figure 12A**). Moreover, 50 nM E2 administration induced estrogen-receptor α (ERα) activity, detected by luciferase reporter assay using luciferase reporter plasmid ERE-Luc in LPO-treated AML12 and HepG2 cells (**Figure 12B**). This E2-induced transcriptional program is mediated by the estrogen receptor alpha (ERα), which is expressed in both untreated and LPO-induced hepatocytes, as determined by western blot analysis (**Figure 12C**).

E2 administration abrogated the LDs accumulation induced by LPO (**Figure 12D**) and concomitantly reduced the ROS levels in both WA01 and WA09-derived HLCs (**Figure 12E**). Moreover, the higher levels of ROS induced by LPO administration in AML12 and HepG2 cells is impaired following treatment with E2, as demonstrated by CellRox measurement (**Figure 12F,G**).

These results suggest that the "gender-relevant phenotype" is influenced by the presence of estrogens rather than by the genetic background of the HLCs, since both WA01 and WA09 cells showed a comparable response to E2. Importantly, these results confirmed the potential protective role of estrogens in counteracting NAFLD progression.

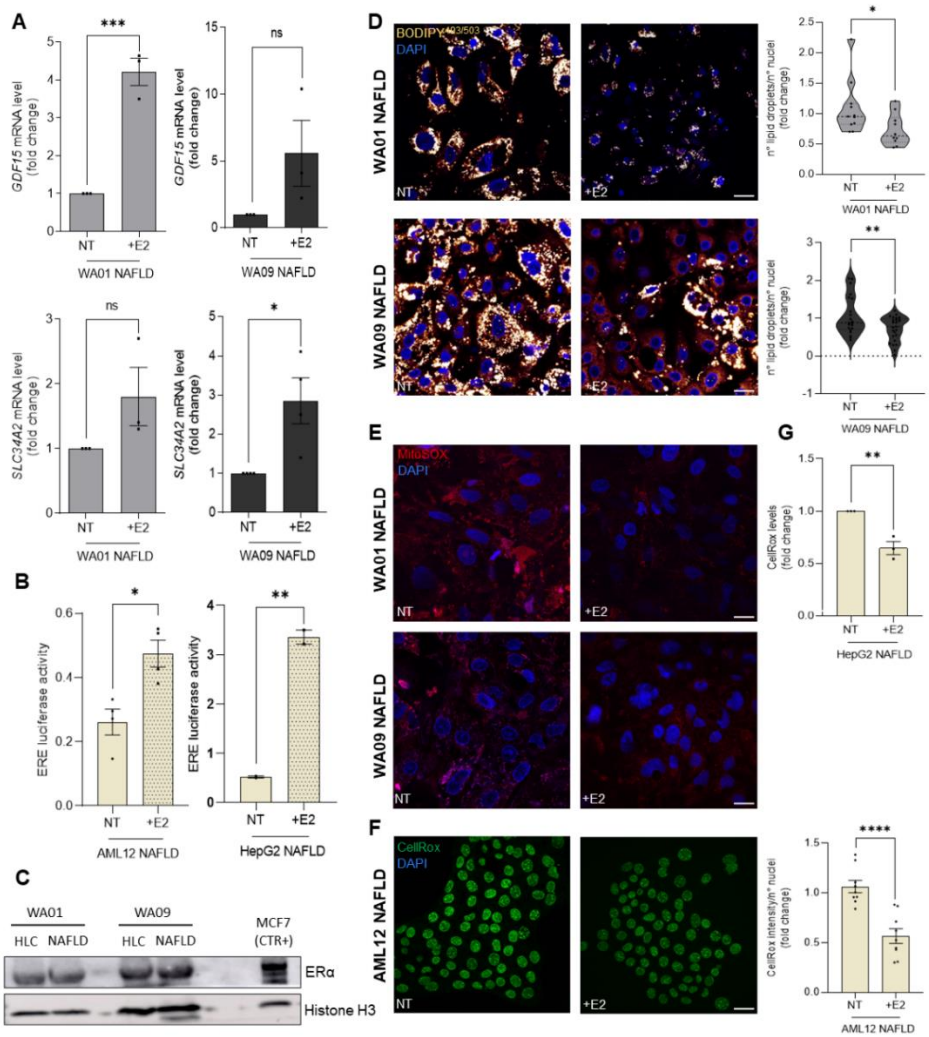

Figure 12. Estrogens reduce LDs accumulation and oxidative stress in steatotic cells. (**A**) LPO-treated WA01, WA09 cells were cultured with or without 1 nM of 17β-estradiol (E2) for 48 hours and subjected to qRT-PCR using the assays described in the figure. Data represent means ± SEM. Student's t test *p < 0.05; **p < 0.01; ***p < 0.001. Each dot represents a biological replicate. (**B**) LPO-treated AML12, HepG2 were cultured with or without 50 nM of 17β-estradiol (E2) for 48 hours and subjected to ERE-luciferase reporter assay. Data represent means ± SEM. Student's t test *p < 0.05; Each dot represents a biological replicate. (**C**) HLCs and LPO-exposed WA01 and WA09 cells were subjected to western blot analysis with the antibody indicated. ER+ MCF7 breast cancer cell line is used as positive control (CTR+) for estrogen receptor alpha (ERα) expression. The Histone H_3 is used as protein loading control normalizer. (**D**) LPO-treated WA01, WA09 cells were cultured with or without 1 nM of 17β-estradiol (E2) for 48 hours and subjected to confocal analysis. Representative pictures of BODIPY$^{493/503}$ stained cells are shown (orange/yellow: LDs; blue: DAPI, nuclei). Quantification of BODIPY spots/cell was reported. Scale bar, 10 μm. (**E**) LPO-treated WA01, WA09 cells were cultured with or without 1 nM of 17β-estradiol (E2) for 48 hours and subjected to confocal analysis. Representative pictures of MitoSOX stained cells are shown (red: MitoSOX; blue: DAPI, nuclei). Scale bar, 10 μm. (**F**) LPO-treated AML12 cells were cultured with or without 50 nM of 17β-estradiol (E2) for 48 hours and subjected to confocal analysis. Representative pictures of CellRox stained cells are shown (Green: CellRox; blue: DAPI, nuclei). Quantification of CellRox intensity was reported. Scale bar, 10 μm. (**G**) Intracellular ROS levels were measured CellRox staining in LPO-treated HepG2 cells cultured with or without 50 nM of 17β-estradiol (E2) for 48 hours. Each dot represents a biological replicate. Data represent means ± SEMs. Student's t test **p < 0.01.

Trx2 inhibition reverts estrogen-mediated ROS buffering

To investigate how E2 can modulate the LPO-induced steatotic phenotype in *in vitro* models, we explored the potential involvement of antioxidant systems that have been reported to be under estrogen control.

First, we postulated that nuclear factor erythroid 2–related factor 2 (NRF2), whose activation is significantly higher in females than in males and is regulated by sex hormones, could be the cause of the antioxidant effects of E2 [255]. Unfortunately, we did not observe a modulation of NRF2 and NRF2-dependent gene (i.e., NQO1) mRNA levels, whose activation is an indicator of nuclear translocation and transcriptional activity of NRF2, in LPO-treated WA01 and WA09 cells in the presence of E2 (**Figure 13A**).

Therefore, we investigated a different antioxidant mechanism that is known to be regulated by estrogens. Based on this, we hypothesized that thioredoxin-2 (Trx2), which is part of the mitochondrial thioredoxin system and is known to be affected by E2 [256], could mediate the ROS buffering effects. In line with this hypothesis, treatment with E2 determined an increase in Trx2 mRNA and protein levels when compared to untreated condition in LPO-induced steatotic WA01 and WA09 HLCs (**Figure 13B**).

To further confirm that the anti-NAFLD effect exerted by E2 could be in part mediated by Trx2 system, we used auranofin, a drug approved for the treatment of rheumatoid arthritis that has been reported to impair Trx2 antioxidant system [257]. Pretreatment of steatotic WA01, WA09, AML12 and HepG2 cells with auranofin prior to E2 administration, reverted the antioxidant effect previously reported for E2, as determined by the increase of mitochondrial and cytoplasmic ROS levels (**Figure 13C,D**).

It should be noted, however, that the administration of auranofin into LPO-exposed cells is nonetheless an oxidative stress for the cells, suggesting that auranofin could have a pro-oxidant effect either by acting directly on the Trx2 system or by affecting other redox control mechanisms.

These data demonstrate that E2 have an antioxidant capacity and could therefore interfere with NAFLD progression through the activation of the Trx2 antioxidant mechanism, a phenomenon reversed by the addition of auranofin.

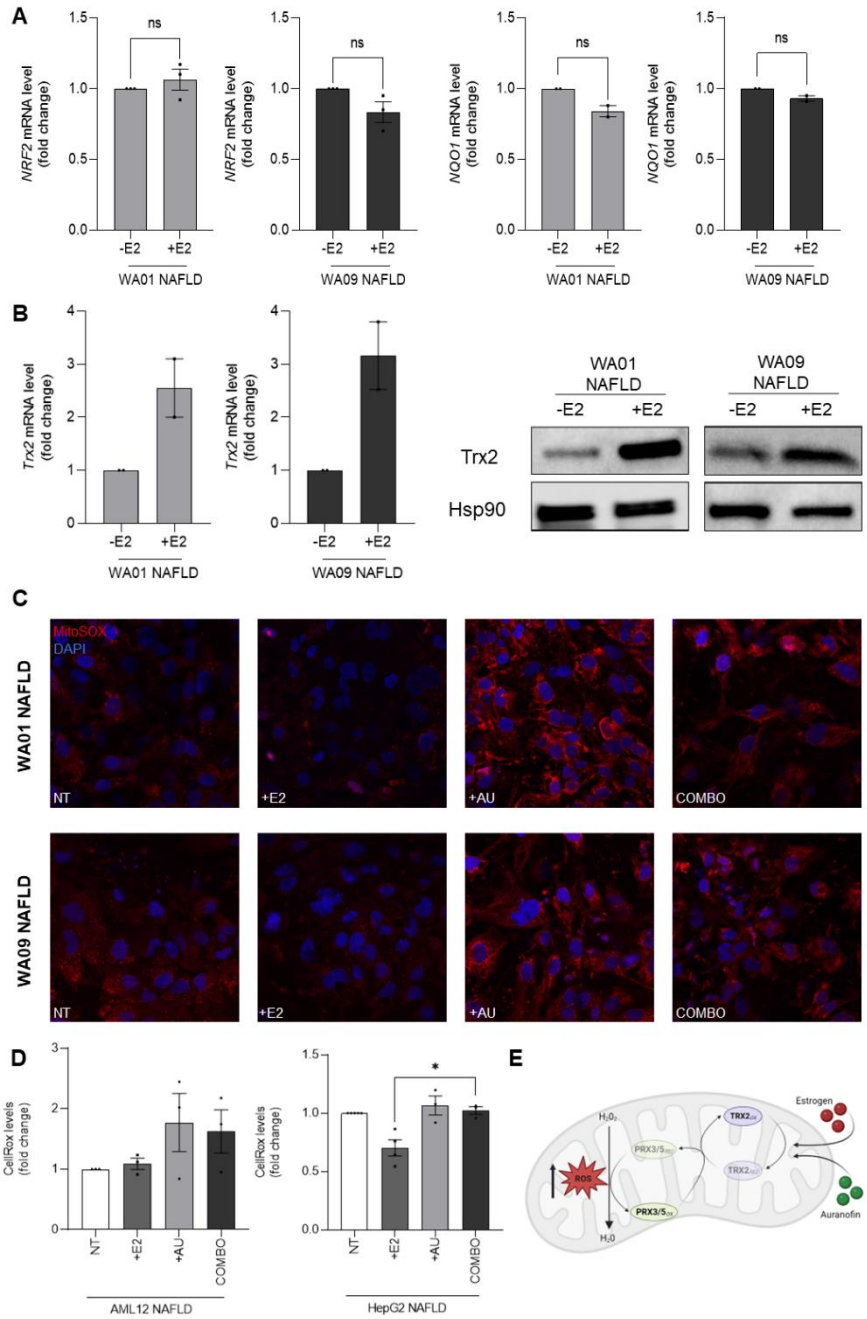

Figure 13. Trx2 inhibition reverts estrogen-mediated ROS buffering. (A) LPO-treated WA01, WA09 cells were cultured with or without 1 nM of 17β-estradiol (E2) for 48 hours and subjected to qRT-PCR using the assays described in the figure. Data represent means ± SEM. Student's t test, non-significant (ns). Each dot represents a biological replicate. (**B**) LPO-treated WA01, WA09 cells were cultured with or without 1 nM of 17β-estradiol (E2) for 48 hours and subjected to qRT-PCR and western blotting analysis using the assays described in the figure. Data represent means ± SEM. (**C**) LPO-treated WA01, WA09 cells were cultured with or without 1 nM of 17β-estradiol (E2) and 500 nM of auranofin (AU) and in combo condition for 48 hours and subjected to confocal analysis. Representative pictures of MitoSOX stained cells are shown (Red: MitoSOX; blue: DAPI, nuclei). (**D**) Intracellular ROS levels were measured with CellRox probe in LPO-treated AML12 and HepG2 cells cultured with 50 nM of 17β-estradiol (E2) and 250 nM of auranofin (AU) and in combo condition for 48 hours. Each dot represents a biological replicate. Data represent means ± SEMs. Student's t test *p < 0.05**.** (**E**) Schematic representation of the mitochondrial Trx2 antioxidant mechanism activated by estrogen and inhibited by auranofin.

Trx2 expression profile in a cohort of NAFLD patients

Finally, to investigate the clinical relevance of our findings, we evaluated whether Trx2 expression correlates with different stage of NAFLD progression and could be associated with NAFLD emergence. Using a transcriptomic approach (GSE163211), Subudhi S. et al. have profiled 795 genes potentially involved in NAFLD initiation/progression in the liver tissues derived from 318 patients (243 females and 75 males), which were categorized into 4 distinct phenotypes: normal liver histology (Normal), steatosis only (Steatosis), non-alcoholic steatohepatitis without fibrosis (NASH_F0), and NASH with fibrosis stage 1-4 (NASH_F1_F4) [258].

Among the genes analyzed, we extrapolated the expression levels of the TXN2 mRNA (another alias gene name for the Trx2 protein) of the 318 liver samples. Taking into consideration only the female branch of the cohort, we subdivided the liver specimens into two groups younger<50 and older≥50, considering 50 years old as the threshold for discriminating the pre to post menopause passage. The GSE163211 dataset was analyzed with GEO2R and *R*-program observing that the expression of TXN2 decreases with the progression of the pathology from normal to NASH_F1_F4. Due to the fact that ROS formation is a critical mechanism in the pathology's progression, it is likely that the absence of estrogens levels and the ensuing E2-dependent ROS scavenging processes explain why this decline is more pronounced in the older female group (**Figure 14**).

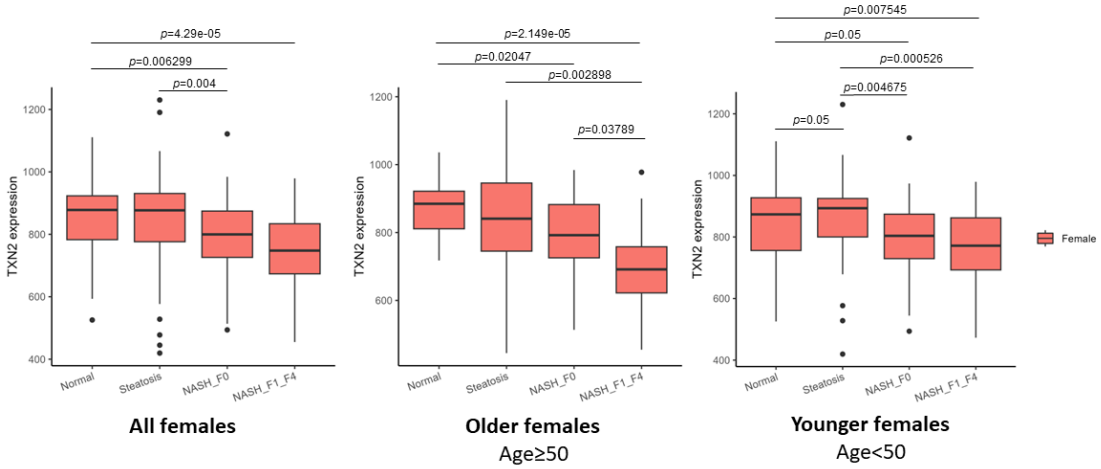

Figure 14. TXN2 mRNA expression levels in liver specimens derived from either normal or NAFLD-bearing patients. Gene expression of TXN2 analyzed with GEO2R and *R*-program in a cohort of normal or NAFLD-bearing patients (GSE163211) divided by age. Wilcox test, $p < 0.05$

DISCUSSION

NAFLD is a global health problem that is associated with the presence of additional comorbidities including obesity, diabetes, cardiovascular and renal disease. Since both genetic and environmental factors contribute to the progression of NAFLD, it is difficult to study the molecular mechanisms underlying the disease and, consequently, to find effective therapeutic approaches. A further aspect complicating the study of NAFLD is the lack of *in vitro* and *in vivo* experimental models capable of recapitulating the complexity of the liver tissue. Currently, *in vivo* murine models serve as the primary research tool for NAFLD because they have demonstrated a higher likelihood of extrapolating findings from studies on the disease's pathophysiology to humans and a more accurate assessment of possible therapeutic targets [259]. A popular *in vivo* model reported in the literature involves feeding C57BL/6 mice two distinct diets: a high-fat (HFD) diet and a ketogenic (KD) diet. This promotes the development of hepatic steatosis, which can lead to fibrosis [260].

Currently, *in vitro* models also represent a suitable alternative for the study of NAFLD, due to the creation of increasingly sophisticated models capable of recapitulating the various distinctive features of the disease. In recent years, the main *in vitro* models for studying NAFLD have mainly used hESC or hiPSC capable of differentiating into the desired cell type with a phenotype similar to the primary cell lines. An example of this strategy is the *in vitro* model used in this thesis, which gives HLCs obtained from male WA01 and female WA09 hESC a cocktail of compounds consisting of LPO. LPO cocktail generates hepatic steatosis, reduces mitochondrial function and increases ROS in HLCs, without compromising cell viability. A further steatotic model used in this thesis is based on the induction of two immortalized liver cell lines called HepG2, hepatocarcinoma cells, and AML12, murine liver cells. We observed the same outcomes on HLCs after treating these cells with LPO, improving a preclinical model for studying NAFLD and proposing new *in vitro* models for studying this clinical condition.

Although such *in vitro* cell models show promising results, it is not easy to find optimal culture conditions for 2D monocultures, which are not able to mimic the complexity of the pathological of NAFLD *in vivo* where, in addition to hepatocytes, other cells of the liver tissue also play a key role. An improvement on this system is provided by 2D co-cultures, which typically involve two or more cell types and are therefore able to represent liver tissue more faithfully. A multidisciplinary approach to i*n vitro* models is the development of much more complex solutions than conventional 2D cultures, like three-dimensional (3D) models and liver-on-a-chip platforms [259]. An example is the

3D spheroid model of PHH, whose exposure to free fatty acids (e.g. palmitate and oleate) and insulin induces lipid accumulation and insulin resistance over a period of about 21 days. The advantages of 3D systems of PHH are represented by the possibility to culture them for up to 3 weeks, allowing experiments with repeated exposure, although the development of such systems is still in the early stages of study [235]. Moreover, 3D models are a valuable tool because they better mimic the phenotype of the organ in vivo and advance our understanding of the disease by containing the different types of liver cells in a controlled microenvironment [259].

Oxidative stress is one of the determining factors in the development and progression of NAFLD. An impairment of the liver's ability to maintain redox balance causes a range of cellular damage, which underlies the pathogenetic mechanisms of many diseases, including NAFLD.

The lower incidence of NAFLD in pre-menopausal women compared to men and post-menopausal women suggests a possible protective role of estrogen. Besides its role in reproduction and sexual development, estrogen can influence the risk of developing liver diseases and more generally metabolic diseases [261]. In particular, estrogen reduces the susceptibility to steatosis development in liver cells of female mice fed an HFD subjected to ovariectomy [262]. Moreover, the deletion of ERα in western-type diet fed female and male mice reduced the ability of isolated hepatocytes to internalize high-density lipoprotein (HDL), although female mice displayed increased cholesterol and HDL serum levels, thus underlying an ERα-independent sex difference [263]. Studies show that estrogens regulate the activity of a series of enzymes involved in *de novo* synthesis and oxidation of fatty acids in the brain, hence affecting lipid metabolism [264]. Furthermore, it has been noted in the literature that the prevalence of metabolic syndrome rises with menopause, most likely as a secondary effect of the metabolic reprogramming from central fat redistribution induced by reduced levels of estrogen [265].

In addition, estrogen can reduce oxidative stress in certain contexts such as in the central nervous system (CNS): indeed, by inducing neurotoxicity in the CNS through ethanol treatment, observed an increase in oxidative stress that can be suppressed by estrogen administration. In the context of cardiovascular diseases, estrogen also plays a protective role; in fact, the onset of these diseases is much higher in men and post-menopausal women; specifically, E2 reduces ROS production and protects against oxidative stress by increasing the activation of antioxidant mechanisms, such as NRF2 pathway [266]. We verified that E2 administration lowers ROS levels linked to NAFLD induction in our experimental models, preventing or postponing the

disease's progression and adding more evidence to the theory that E2 regulates oxidative stress and lipid accumulation. However, estrogen do not always play a protective role against oxidative stress and their presence has been reported to the opposite effect leading to an increase in ROS levels. Indeed, in this regard, a study [267] conducted on ovarian adenocarcinoma cells showed that estrogen increase ROS levels, an effect reversed by the addition of the antioxidant N-acetyl-L-cysteine [268].

It might also be interesting to examine the role that estrogen-mediated metabolic reprogramming plays in the onset and progression of NAFLD, since this condition is thought to be a hepatic manifestation of the metabolic syndrome.

Our studies show that estrogen possesses a protective effect against the NAFL-associated manifestations induced by LPO administration, which appears to be mediated by the activation of the antioxidant mechanism of Trx2, a mitochondrial ROS scavenger. Importantly, the regulation of Trx2 by estrogens appears to be a key mechanism in the prevention of oxidative damage also in other pathological conditions: a study in brain-injured mice found that estrogen protects the mice by activating Trx2 and lowering ROS levels and mitochondrial damage [269, 270]. Furthermore, it has been reported that Trx2 gene expression in the uterus is regulated *in vivo* by sex hormones [256].

Finally, because sex has an undeniable impact on NAFLD incidence in humans, with a male bias in global incidence, and sex hormones have been shown to contribute to this bias, it should be noted that there are only a few sex-based comparison approaches available. Indeed, most studies conducted so far in the field of NAFLD and HCC have been performed in male animals whereas the female sex is still highly underrepresented. Moreover, sex is often confused with gender making even harder for researchers that want to study this clinically relevant area of research to gain useful information. Such approach is fundamental not only for the elucidation of mechanisms implicated in NAFLD pathogenesis, but also for understanding and improvement of existing and novel treatment strategies [271].

An important limitation of this thesis is the lack of an *in vivo* study validation. In particular, the evaluation of the effect of estrogens in male and female mice subjected to NAFLD initiation/progression protocol would be highly valuable. In such experimental approach, we could also exploit the interference with the Trx2 system, since auranofin has been already administered *in vivo* [272]. As a future plan, to better dissect the differences between men and women related to NAFLD incidence, we should use a NAFLD inducing protocol in male and female mice, in the presence or

absence of estrogens. Although this sounds particularly challenging, it could be achieved by treating OVX female mice with or without estrogen while feeding them on HFD. Similarly, we could expose HFD-fed male mice to estrogen administration.

Taken together, although some of the findings should be recapitulated in more complex models, we have demonstrated an important estrogen-dependent redox homeostatic control which may be important for NAFLD initiation and progression (Figure 15, **Graphical Abstract**).

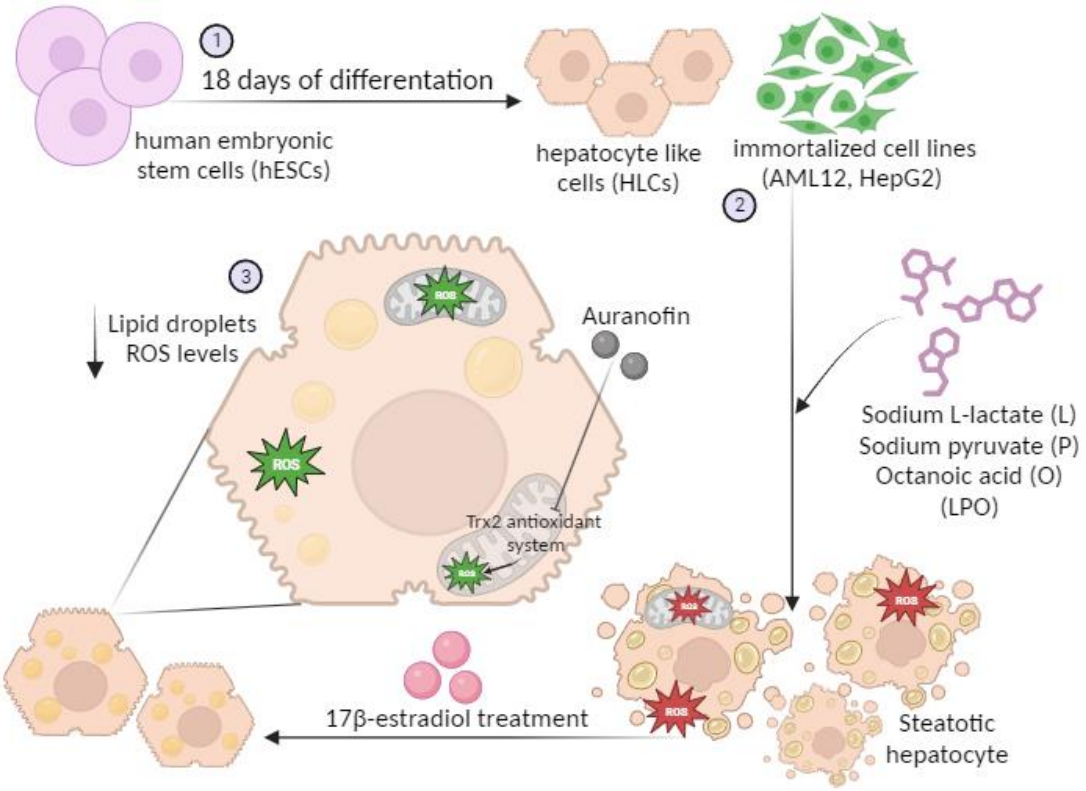

Figure 15. Graphical abstract of the study. (1) Human embryonic stem cells (hESCs) were differentiated into hepatocyte like cells (HLCs) using an 18-day differentiation protocol [249]; **(2)** HLCs and hepatic immortalized cell lines (AML12, HepG2) were then treated with sodium L-lactate (L), sodium pyruvate (P) and octanoic acid (O), a protocol of induction called LPO. LPO administration induces distinct steatotic traits, such as the accumulation of lipid droplets and an increase in reactive oxygen species (ROS) levels. **(3)** Treatment with 17β-estradiol results in a reduction of the distinctive traits of NAFLD through the activation of the mitochondrial antioxidant mechanism of thioredoxin 2 (Trx2), which is inhibited by the administration of auranofin.

BIBLIOGRAPHY

[1] Kalra A, Yetiskul E, Wehrle CJ, Tuma F. Physiology, Liver.
[2] Si-Tayeb K, Lemaigre FP, Duncan SA. Organogenesis and development of the liver. Dev Cell 2010;18:175-189.
[3] Vernon H, Wehrle CJ, Alia VSK, Kasi A. Anatomy, Abdomen and Pelvis: Liver.
[4] Trefts E, Gannon M, Wasserman DH. The liver. Curr Biol 2017;27:R1147-R1151.
[5] Asrani SK, Devarbhavi H, Eaton J, Kamath PS. Burden of liver diseases in the world. J Hepatol 2019;70:151-171.
[6] Lozano R, Naghavi M, Foreman K, Lim S, Shibuya K, Aboyans V, et al. Global and regional mortality from 235 causes of death for 20 age groups in 1990 and 2010: a systematic analysis for the Global Burden of Disease Study 2010. Lancet 2012;380:2095-2128.
[7] Ahmed A, Wong RJ, Harrison SA. Nonalcoholic Fatty Liver Disease Review: Diagnosis, Treatment, and Outcomes. Clin Gastroenterol Hepatol 2015;13:2062-2070.
[8] Machado MV, Diehl AM. Pathogenesis of Nonalcoholic Steatohepatitis. Gastroenterology 2016;150:1769-1777.
[9] Browning JD, Szczepaniak LS, Dobbins R, Nuremberg P, Horton JD, Cohen JC, et al. Prevalence of hepatic steatosis in an urban population in the United States: impact of ethnicity. Hepatology 2004;40:1387-1395.
[10] Ahmed MH, Husain NE, Almobarak AO. Nonalcoholic Fatty liver disease and risk of diabetes and cardiovascular disease: what is important for primary care physicians? J Family Med Prim Care 2015;4:45-52.
[11] Jackson KG, Way GW, Zhou H. Bile acids and sphingolipids in non-alcoholic fatty liver disease. Chin Med J (Engl) 2022;135:1163-1171.
[12] Riazi K, Azhari H, Charette JH, Underwood FE, King JA, Afshar EE, et al. The prevalence and incidence of NAFLD worldwide: a systematic review and meta-analysis. Lancet Gastroenterol Hepatol 2022;7:851-861.
[13] Wong VW, Ekstedt M, Wong GL, Hagström H. Changing epidemiology, global trends and implications for outcomes of NAFLD. J Hepatol 2023;79:842-852.
[14] Younossi ZM, Koenig AB, Abdelatif D, Fazel Y, Henry L, Wymer M. Global epidemiology of nonalcoholic fatty liver disease-Meta-analytic assessment of prevalence, incidence, and outcomes. Hepatology 2016;64:73-84.
[15] Armstrong MJ, Houlihan DD, Bentham L, Shaw JC, Cramb R, Olliff S, et al. Presence and severity of non-alcoholic fatty liver disease in a large prospective primary care cohort. J Hepatol 2012;56:234-240.
[16] Kanwal F, Kramer JR, Duan Z, Yu X, White D, El-Serag HB. Trends in the Burden of Nonalcoholic Fatty Liver Disease in a United States Cohort of Veterans. Clin Gastroenterol Hepatol 2016;14:301-308.e301-302.
[17] Rinella M, Charlton M. The globalization of nonalcoholic fatty liver disease: Prevalence and impact on world health. Hepatology 2016;64:19-22.
[18] Hamaguchi M, Kojima T, Takeda N, Nakagawa T, Taniguchi H, Fujii K, et al. The metabolic syndrome as a predictor of nonalcoholic fatty liver disease. Ann Intern Med 2005;143:722-728.
[19] Yun KE, Nam GE, Lim J, Park HS, Chang Y, Jung HS, et al. Waist Gain Is Associated with a Higher Incidence of Nonalcoholic Fatty Liver Disease in Korean Adults: A Cohort Study. PLoS One 2016;11:e0158710.
[20] Fan JG, Zhu J, Li XJ, Chen L, Li L, Dai F, et al. Prevalence of and risk factors for fatty liver in a general population of Shanghai, China. J Hepatol 2005;43:508-514.
[21] Eguchi Y, Hyogo H, Ono M, Mizuta T, Ono N, Fujimoto K, et al. Prevalence and associated metabolic factors of nonalcoholic fatty liver disease in the general

population from 2009 to 2010 in Japan: a multicenter large retrospective study. J Gastroenterol 2012;47:586-595.
[22] Hu X, Huang Y, Bao Z, Wang Y, Shi D, Liu F, et al. Prevalence and factors associated with nonalcoholic fatty liver disease in Shanghai work-units. BMC Gastroenterol 2012;12:123.
[23] Wang Z, Xu M, Hu Z, Hultström M, Lai E. Sex-specific prevalence of fatty liver disease and associated metabolic factors in Wuhan, south central China. Eur J Gastroenterol Hepatol 2014;26:1015-1021.
[24] Bruno S, Maisonneuve P, Castellana P, Rotmensz N, Rossi S, Maggioni M, et al. Incidence and risk factors for non-alcoholic steatohepatitis: prospective study of 5408 women enrolled in Italian tamoxifen chemoprevention trial. BMJ 2005;330:932.
[25] Devarbhavi H, Asrani SK, Arab JP, Nartey YA, Pose E, Kamath PS. Global burden of liver disease: 2023 update. J Hepatol 2023;79:516-537.
[26] Peverill W, Powell LW, Skoien R. Evolving concepts in the pathogenesis of NASH: beyond steatosis and inflammation. Int J Mol Sci 2014;15:8591-8638.
[27] Leamy AK, Egnatchik RA, Young JD. Molecular mechanisms and the role of saturated fatty acids in the progression of non-alcoholic fatty liver disease. Prog Lipid Res 2013;52:165-174.
[28] Bugianesi E, Moscatiello S, Ciaravella MF, Marchesini G. Insulin resistance in nonalcoholic fatty liver disease. Curr Pharm Des 2010;16:1941-1951.
[29] Guilherme A, Virbasius JV, Puri V, Czech MP. Adipocyte dysfunctions linking obesity to insulin resistance and type 2 diabetes. Nat Rev Mol Cell Biol 2008;9:367-377.
[30] Cusi K. Role of insulin resistance and lipotoxicity in non-alcoholic steatohepatitis. Clin Liver Dis 2009;13:545-563.
[31] Kirpich IA, Marsano LS, McClain CJ. Gut-liver axis, nutrition, and non-alcoholic fatty liver disease. Clin Biochem 2015;48:923-930.
[32] Yilmaz Y. Review article: is non-alcoholic fatty liver disease a spectrum, or are steatosis and non-alcoholic steatohepatitis distinct conditions? Aliment Pharmacol Ther 2012;36:815-823.
[33] Lewis GF, Carpentier A, Adeli K, Giacca A. Disordered fat storage and mobilization in the pathogenesis of insulin resistance and type 2 diabetes. Endocr Rev 2002;23:201-229.
[34] Ipsen DH, Lykkesfeldt J, Tveden-Nyborg P. Molecular mechanisms of hepatic lipid accumulation in non-alcoholic fatty liver disease. Cell Mol Life Sci 2018;75:3313-3327.
[35] Lambert JE, Ramos-Roman MA, Browning JD, Parks EJ. Increased de novo lipogenesis is a distinct characteristic of individuals with nonalcoholic fatty liver disease. Gastroenterology 2014;146:726-735.
[36] George J, Liddle C. Nonalcoholic fatty liver disease: pathogenesis and potential for nuclear receptors as therapeutic targets. Mol Pharm 2008;5:49-59.
[37] Schwarz JM, Linfoot P, Dare D, Aghajanian K. Hepatic de novo lipogenesis in normoinsulinemic and hyperinsulinemic subjects consuming high-fat, low-carbohydrate and low-fat, high-carbohydrate isoenergetic diets. Am J Clin Nutr 2003;77:43-50.
[38] Postic C, Girard J. Contribution of de novo fatty acid synthesis to hepatic steatosis and insulin resistance: lessons from genetically engineered mice. J Clin Invest 2008;118:829-838.
[39] Lee Y, Hirose H, Ohneda M, Johnson JH, McGarry JD, Unger RH. Beta-cell lipotoxicity in the pathogenesis of non-insulin-dependent diabetes mellitus of obese rats: impairment in adipocyte-beta-cell relationships. Proc Natl Acad Sci U S A 1994;91:10878-10882.
[40] Grefhorst A, van de Peppel IP, Larsen LE, Jonker JW, Holleboom AG. The Role of Lipophagy in the Development and Treatment of Non-Alcoholic Fatty Liver Disease. Front Endocrinol (Lausanne) 2020;11:601627.

[41] Alfadda AA, Sallam RM. Reactive oxygen species in health and disease. J Biomed Biotechnol 2012;2012:936486.
[42] Annesley SJ, Fisher PR. Mitochondria in Health and Disease. Cells 2019;8.
[43] Papa S, Martino PL, Capitanio G, Gaballo A, De Rasmo D, Signorile A, et al. The oxidative phosphorylation system in mammalian mitochondria. Adv Exp Med Biol 2012;942:3-37.
[44] Peoples JN, Saraf A, Ghazal N, Pham TT, Kwong JQ. Mitochondrial dysfunction and oxidative stress in heart disease. Exp Mol Med 2019;51:1-13.
[45] Snezhkina AV, Kudryavtseva AV, Kardymon OL, Savvateeva MV, Melnikova NV, Krasnov GS, et al. ROS Generation and Antioxidant Defense Systems in Normal and Malignant Cells. Oxid Med Cell Longev 2019;2019:6175804.
[46] Deguise MO, Pileggi C, De Repentigny Y, Beauvais A, Tierney A, Chehade L, et al. SMN Depleted Mice Offer a Robust and Rapid Onset Model of Nonalcoholic Fatty Liver Disease. Cell Mol Gastroenterol Hepatol 2021;12:354-377.e353.
[47] Han J, Li E, Chen L, Zhang Y, Wei F, Liu J, et al. The CREB coactivator CRTC2 controls hepatic lipid metabolism by regulating SREBP1. Nature 2015;524:243-246.
[48] Hwang-Bo H, Jeong JW, Han MH, Park C, Hong SH, Kim GY, et al. Auranofin, an inhibitor of thioredoxin reductase, induces apoptosis in hepatocellular carcinoma Hep3B cells by generation of reactive oxygen species. Gen Physiol Biophys 2017;36:117-128.
[49] Li Z, Berk M, McIntyre TM, Gores GJ, Feldstein AE. The lysosomal-mitochondrial axis in free fatty acid-induced hepatic lipotoxicity. Hepatology 2008;47:1495-1503.
[50] Rolo AP, Teodoro JS, Palmeira CM. Role of oxidative stress in the pathogenesis of nonalcoholic steatohepatitis. Free Radic Biol Med 2012;52:59-69.
[51] Schuster S, Cabrera D, Arrese M, Feldstein AE. Triggering and resolution of inflammation in NASH. Nat Rev Gastroenterol Hepatol 2018;15:349-364.
[52] Daryabor G, Atashzar MR, Kabelitz D, Meri S, Kalantar K. The Effects of Type 2 Diabetes Mellitus on Organ Metabolism and the Immune System. Front Immunol 2020;11:1582.
[53] Albhaisi S, Noureddin M. Current and Potential Therapies Targeting Inflammation in NASH. Front Endocrinol (Lausanne) 2021;12:767314.
[54] Mridha AR, Wree A, Robertson AAB, Yeh MM, Johnson CD, Van Rooyen DM, et al. NLRP3 inflammasome blockade reduces liver inflammation and fibrosis in experimental NASH in mice. J Hepatol 2017;66:1037-1046.
[55] Hardy T, Oakley F, Anstee QM, Day CP. Nonalcoholic Fatty Liver Disease: Pathogenesis and Disease Spectrum. Annu Rev Pathol 2016;11:451-496.
[56] Krenkel O, Tacke F. Liver macrophages in tissue homeostasis and disease. Nat Rev Immunol 2017;17:306-321.
[57] Roh YS, Seki E. Toll-like receptors in alcoholic liver disease, non-alcoholic steatohepatitis and carcinogenesis. J Gastroenterol Hepatol 2013;28 Suppl 1:38-42.
[58] Heyens LJM, Busschots D, Koek GH, Robaeys G, Francque S. Liver Fibrosis in Non-alcoholic Fatty Liver Disease: From Liver Biopsy to Non-invasive Biomarkers in Diagnosis and Treatment. Front Med (Lausanne) 2021;8:615978.
[59] Bataller R, Brenner DA. Liver fibrosis. J Clin Invest 2005;115:209-218.
[60] Hyysalo J, Stojkovic I, Kotronen A, Hakkarainen A, Sevastianova K, Makkonen J, et al. Genetic variation in PNPLA3 but not APOC3 influences liver fat in non-alcoholic fatty liver disease. J Gastroenterol Hepatol 2012;27:951-956.
[61] Sookoian S, Pirola CJ. Meta-analysis of the influence of I148M variant of patatin-like phospholipase domain containing 3 gene (PNPLA3) on the susceptibility and histological severity of nonalcoholic fatty liver disease. Hepatology 2011;53:1883-1894.
[62] Anstee QM, Day CP. The genetics of NAFLD. Nat Rev Gastroenterol Hepatol 2013;10:645-655.

[63] BasuRay S, Smagris E, Cohen JC, Hobbs HH. The PNPLA3 variant associated with fatty liver disease (I148M) accumulates on lipid droplets by evading ubiquitylation. Hepatology 2017;66:1111-1124.
[64] Smagris E, Gilyard S, BasuRay S, Cohen JC, Hobbs HH. Inactivation of Tm6sf2, a Gene Defective in Fatty Liver Disease, Impairs Lipidation but Not Secretion of Very Low Density Lipoproteins. J Biol Chem 2016;291:10659-10676.
[65] Kozlitina J, Smagris E, Stender S, Nordestgaard BG, Zhou HH, Tybjærg-Hansen A, et al. Exome-wide association study identifies a TM6SF2 variant that confers susceptibility to nonalcoholic fatty liver disease. Nat Genet 2014;46:352-356.
[66] Tanaka Y, Shimanaka Y, Caddeo A, Kubo T, Mao Y, Kubota T, et al. LPIAT1/MBOAT7 depletion increases triglyceride synthesis fueled by high phosphatidylinositol turnover. Gut 2021;70:180-193.
[67] Huh Y, Cho YJ, Nam GE. Recent Epidemiology and Risk Factors of Nonalcoholic Fatty Liver Disease. J Obes Metab Syndr 2022;31:17-27.
[68] Wainwright P, Byrne CD. Bidirectional Relationships and Disconnects between NAFLD and Features of the Metabolic Syndrome. Int J Mol Sci 2016;17:367.
[69] Byrne CD, Targher G. NAFLD: a multisystem disease. J Hepatol 2015;62:S47-64.
[70] Younossi Z, Anstee QM, Marietti M, Hardy T, Henry L, Eslam M, et al. Global burden of NAFLD and NASH: trends, predictions, risk factors and prevention. Nat Rev Gastroenterol Hepatol 2018;15:11-20.
[71] Raza S, Rajak S, Upadhyay A, Tewari A, Anthony Sinha R. Current treatment paradigms and emerging therapies for NAFLD/NASH. Front Biosci (Landmark Ed) 2021;26:206-237.
[72] Vilar-Gomez E, Martinez-Perez Y, Calzadilla-Bertot L, Torres-Gonzalez A, Gra-Oramas B, Gonzalez-Fabian L, et al. Weight Loss Through Lifestyle Modification Significantly Reduces Features of Nonalcoholic Steatohepatitis. Gastroenterology 2015;149:367-378.e365; quiz e314-365.
[73] Mathurin P, Hollebecque A, Arnalsteen L, Buob D, Leteurtre E, Caiazzo R, et al. Prospective study of the long-term effects of bariatric surgery on liver injury in patients without advanced disease. Gastroenterology 2009;137:532-540.
[74] Filipovic B, Lukic S, Mijac D, Marjanovic-Haljilji M, Vojnovic M, Bogdanovic J, et al. The New Therapeutic Approaches in the Treatment of Non-Alcoholic Fatty Liver Disease. Int J Mol Sci 2021;22.
[75] Chalasani N, Younossi Z, Lavine JE, Charlton M, Cusi K, Rinella M, et al. The diagnosis and management of nonalcoholic fatty liver disease: Practice guidance from the American Association for the Study of Liver Diseases. Hepatology 2018;67:328-357.
[76] Grundy SM, Cleeman JI, Daniels SR, Donato KA, Eckel RH, Franklin BA, et al. Diagnosis and management of the metabolic syndrome: an American Heart Association/National Heart, Lung, and Blood Institute Scientific Statement. Circulation 2005;112:2735-2752.
[77] Anania C, Perla FM, Olivero F, Pacifico L, Chiesa C. Mediterranean diet and nonalcoholic fatty liver disease. World J Gastroenterol 2018;24:2083-2094.
[78] Di Daniele N, Noce A, Vidiri MF, Moriconi E, Marrone G, Annicchiarico-Petruzzelli M, et al. Impact of Mediterranean diet on metabolic syndrome, cancer and longevity. Oncotarget 2017;8:8947-8979.
[79] (EASL) EAftSotL, (EASD) EAftSoD, (EASO) EAftSoO. EASL-EASD-EASO Clinical Practice Guidelines for the management of non-alcoholic fatty liver disease. J Hepatol 2016;64:1388-1402.
[80] LaMonte MJ, Blair SN, Church TS. Physical activity and diabetes prevention. J Appl Physiol (1985) 2005;99:1205-1213.
[81] Fernández T, Viñuela M, Vidal C, Barrera F. Lifestyle changes in patients with non-alcoholic fatty liver disease: A systematic review and meta-analysis. PLoS One 2022;17:e0263931.

[82] Samuel VT, Shulman GI. Nonalcoholic Fatty Liver Disease as a Nexus of Metabolic and Hepatic Diseases. Cell Metab 2018;27:22-41.
[83] Feige JN, Gelman L, Michalik L, Desvergne B, Wahli W. From molecular action to physiological outputs: peroxisome proliferator-activated receptors are nuclear receptors at the crossroads of key cellular functions. Prog Lipid Res 2006;45:120-159.
[84] Francque S, Verrijken A, Caron S, Prawitt J, Paumelle R, Derudas B, et al. PPARα gene expression correlates with severity and histological treatment response in patients with non-alcoholic steatohepatitis. J Hepatol 2015;63:164-173.
[85] Zarei M, Barroso E, Palomer X, Dai J, Rada P, Quesada-López T, et al. Hepatic regulation of VLDL receptor by PPARβ/δ and FGF21 modulates non-alcoholic fatty liver disease. Mol Metab 2018;8:117-131.
[86] Bajaj M, Suraamornkul S, Piper P, Hardies LJ, Glass L, Cersosimo E, et al. Decreased plasma adiponectin concentrations are closely related to hepatic fat content and hepatic insulin resistance in pioglitazone-treated type 2 diabetic patients. J Clin Endocrinol Metab 2004;89:200-206.
[87] Bril F, Kalavalapalli S, Clark VC, Lomonaco R, Soldevila-Pico C, Liu IC, et al. Response to Pioglitazone in Patients With Nonalcoholic Steatohepatitis With vs Without Type 2 Diabetes. Clin Gastroenterol Hepatol 2018;16:558-566.e552.
[88] Gawrieh S, Noureddin M, Loo N, Mohseni R, Awasty V, Cusi K, et al. Saroglitazar, a PPAR-α/γ Agonist, for Treatment of NAFLD: A Randomized Controlled Double-Blind Phase 2 Trial. Hepatology 2021;74:1809-1824.
[89] Watanabe M, Houten SM, Wang L, Moschetta A, Mangelsdorf DJ, Heyman RA, et al. Bile acids lower triglyceride levels via a pathway involving FXR, SHP, and SREBP-1c. J Clin Invest 2004;113:1408-1418.
[90] Ma K, Saha PK, Chan L, Moore DD. Farnesoid X receptor is essential for normal glucose homeostasis. J Clin Invest 2006;116:1102-1109.
[91] Aguilar-Olivos NE, Carrillo-Córdova D, Oria-Hernández J, Sánchez-Valle V, Ponciano-Rodríguez G, Ramírez-Jaramillo M, et al. The nuclear receptor FXR, but not LXR, up-regulates bile acid transporter expression in non-alcoholic fatty liver disease. Ann Hepatol 2015;14:487-493.
[92] Younossi ZM, Ratziu V, Loomba R, Rinella M, Anstee QM, Goodman Z, et al. Obeticholic acid for the treatment of non-alcoholic steatohepatitis: interim analysis from a multicentre, randomised, placebo-controlled phase 3 trial. Lancet 2019;394:2184-2196.
[93] Ratziu V, Sanyal AJ, Loomba R, Rinella M, Harrison S, Anstee QM, et al. REGENERATE: Design of a pivotal, randomised, phase 3 study evaluating the safety and efficacy of obeticholic acid in patients with fibrosis due to nonalcoholic steatohepatitis. Contemp Clin Trials 2019;84:105803.
[94] Ratziu V, Rinella ME, Neuschwander-Tetri BA, Lawitz E, Denham D, Kayali Z, et al. EDP-305 in patients with NASH: A phase II double-blind placebo-controlled dose-ranging study. J Hepatol 2022;76:506-517.
[95] Ratziu V, Harrison SA, Loustaud-Ratti V, Bureau C, Lawitz E, Abdelmalek M, et al. Hepatic and renal improvements with FXR agonist vonafexor in individuals with suspected fibrotic NASH. J Hepatol 2023;78:479-492.
[96] Neuschwander-Tetri BA. Hepatic lipotoxicity and the pathogenesis of nonalcoholic steatohepatitis: the central role of nontriglyceride fatty acid metabolites. Hepatology 2010;52:774-788.
[97] Loomba R, Mohseni R, Lucas KJ, Gutierrez JA, Perry RG, Trotter JF, et al. TVB-2640 (FASN Inhibitor) for the Treatment of Nonalcoholic Steatohepatitis: FASCINATE-1, a Randomized, Placebo-Controlled Phase 2a Trial. Gastroenterology 2021;161:1475-1486.
[98] Wang Y, Yu W, Li S, Guo D, He J. Acetyl-CoA Carboxylases and Diseases. Front Oncol 2022;12:836058.

[99] Bates J, Vijayakumar A, Ghoshal S, Marchand B, Yi S, Kornyeyev D, et al. Acetyl-CoA carboxylase inhibition disrupts metabolic reprogramming during hepatic stellate cell activation. J Hepatol 2020;73:896-905.
[100] Lawitz EJ, Coste A, Poordad F, Alkhouri N, Loo N, McColgan BJ, et al. Acetyl-CoA Carboxylase Inhibitor GS-0976 for 12 Weeks Reduces Hepatic De Novo Lipogenesis and Steatosis in Patients With Nonalcoholic Steatohepatitis. Clin Gastroenterol Hepatol 2018;16:1983-1991.e1983.
[101] Roe ND, Handzlik MK, Li T, Tian R. The Role of Diacylglycerol Acyltransferase (DGAT) 1 and 2 in Cardiac Metabolism and Function. Sci Rep 2018;8:4983.
[102] Li C, Li L, Lian J, Watts R, Nelson R, Goodwin B, et al. Roles of Acyl-CoA:Diacylglycerol Acyltransferases 1 and 2 in Triacylglycerol Synthesis and Secretion in Primary Hepatocytes. Arterioscler Thromb Vasc Biol 2015;35:1080-1091.
[103] Li S, Tan HY, Wang N, Zhang ZJ, Lao L, Wong CW, et al. The Role of Oxidative Stress and Antioxidants in Liver Diseases. Int J Mol Sci 2015;16:26087-26124.
[104] Del Ben M, Polimeni L, Baratta F, Pastori D, Angelico F. The role of nutraceuticals for the treatment of non-alcoholic fatty liver disease. Br J Clin Pharmacol 2017;83:88-95.
[105] Hayes JD, Dinkova-Kostova AT. The Nrf2 regulatory network provides an interface between redox and intermediary metabolism. Trends Biochem Sci 2014;39:199-218.
[106] Bricambert J, Alves-Guerra MC, Esteves P, Prip-Buus C, Bertrand-Michel J, Guillou H, et al. The histone demethylase Phf2 acts as a molecular checkpoint to prevent NAFLD progression during obesity. Nat Commun 2018;9:2092.
[107] Azzimato V, Jager J, Chen P, Morgantini C, Levi L, Barreby E, et al. Liver macrophages inhibit the endogenous antioxidant response in obesity-associated insulin resistance. Sci Transl Med 2020;12.
[108] Tanaka Y, Aleksunes LM, Yeager RL, Gyamfi MA, Esterly N, Guo GL, et al. NF-E2-related factor 2 inhibits lipid accumulation and oxidative stress in mice fed a high-fat diet. J Pharmacol Exp Ther 2008;325:655-664.
[109] Shimozono R, Asaoka Y, Yoshizawa Y, Aoki T, Noda H, Yamada M, et al. Nrf2 activators attenuate the progression of nonalcoholic steatohepatitis-related fibrosis in a dietary rat model. Mol Pharmacol 2013;84:62-70.
[110] Kim W, Kim BG, Lee JS, Lee CK, Yeon JE, Chang MS, et al. Randomised clinical trial: the efficacy and safety of oltipraz, a liver X receptor alpha-inhibitory dithiolethione in patients with non-alcoholic fatty liver disease. Aliment Pharmacol Ther 2017;45:1073-1083.
[111] Izdebska M, Piątkowska-Chmiel I, Korolczuk A, Herbet M, Gawrońska-Grzywacz M, Gieroba R, et al. The beneficial effects of resveratrol on steatosis and mitochondrial oxidative stress in HepG2 cells. Can J Physiol Pharmacol 2017;95:1442-1453.
[112] Liu CW, Huang CC, Hsu CF, Li TH, Tsai YL, Lin MW, et al. SIRT1-dependent mechanisms and effects of resveratrol for amelioration of muscle wasting in NASH mice. BMJ Open Gastroenterol 2020;7.
[113] Faghihzadeh F, Adibi P, Rafiei R, Hekmatdoost A. Resveratrol supplementation improves inflammatory biomarkers in patients with nonalcoholic fatty liver disease. Nutr Res 2014;34:837-843.
[114] Li J, Wang T, Liu P, Yang F, Wang X, Zheng W, et al. Hesperetin ameliorates hepatic oxidative stress and inflammation. Food Funct 2021;12:3898-3918.
[115] Yang JP, Shin JH, Seo SH, Kim SG, Lee SH, Shin EH. Effects of Antioxidants in Reducing Accumulation of Fat in Hepatocyte. Int J Mol Sci 2018;19.
[116] Raso GM, Esposito E, Iacono A, Pacilio M, Cuzzocrea S, Canani RB, et al. Comparative therapeutic effects of metformin and vitamin E in a model of non-alcoholic steatohepatitis in the young rat. Eur J Pharmacol 2009;604:125-131.
[117] Sumida Y, Yoneda M, Seko Y, Takahashi H, Hara N, Fujii H, et al. Role of vitamin E in the treatment of non-alcoholic steatohepatitis. Free Radic Biol Med 2021;177:391-403.

[118] Sanyal AJ, Chalasani N, Kowdley KV, McCullough A, Diehl AM, Bass NM, et al. Pioglitazone, vitamin E, or placebo for nonalcoholic steatohepatitis. N Engl J Med 2010;362:1675-1685.
[119] Ni Y, Nagashimada M, Zhan L, Nagata N, Kobori M, Sugiura M, et al. Prevention and reversal of lipotoxicity-induced hepatic insulin resistance and steatohepatitis in mice by an antioxidant carotenoid, β-cryptoxanthin. Endocrinology 2015;156:987-999.
[120] Brandt A, Hernández-Arriaga A, Kehm R, Sánchez V, Jin CJ, Nier A, et al. Metformin attenuates the onset of non-alcoholic fatty liver disease and affects intestinal microbiota and barrier in small intestine. Sci Rep 2019;9:6668.
[121] Conde de la Rosa L, Vrenken TE, Buist-Homan M, Faber KN, Moshage H. Metformin protects primary rat hepatocytes against oxidative stress-induced apoptosis. Pharmacol Res Perspect 2015;3:e00125.
[122] Colak Y, Hasan B, Erkalma B, Tandon K, Zervos X, Menzo EL, et al. Pathogenetic mechanisms of nonalcoholic fatty liver disease and inhibition of the inflammasome as a new therapeutic target. Clin Res Hepatol Gastroenterol 2021;45:101710.
[123] Yang G, Lee HE, Lee JY. A pharmacological inhibitor of NLRP3 inflammasome prevents non-alcoholic fatty liver disease in a mouse model induced by high fat diet. Sci Rep 2016;6:24399.
[124] Yang Y, Wang H, Kouadir M, Song H, Shi F. Recent advances in the mechanisms of NLRP3 inflammasome activation and its inhibitors. Cell Death Dis 2019;10:128.
[125] Du J, Ma YY, Yu CH, Li YM. Effects of pentoxifylline on nonalcoholic fatty liver disease: a meta-analysis. World J Gastroenterol 2014;20:569-577.
[126] Koca SS, Bahcecioglu IH, Poyrazoglu OK, Ozercan IH, Sahin K, Ustundag B. The treatment with antibody of TNF-alpha reduces the inflammation, necrosis and fibrosis in the non-alcoholic steatohepatitis induced by methionine- and choline-deficient diet. Inflammation 2008;31:91-98.
[127] Bennett RG, Simpson RL, Hamel FG. Serelaxin increases the antifibrotic action of rosiglitazone in a model of hepatic fibrosis. World J Gastroenterol 2017;23:3999-4006.
[128] Al Attar A, Antaramian A, Noureddin M. Review of galectin-3 inhibitors in the treatment of nonalcoholic steatohepatitis. Expert Rev Clin Pharmacol 2021;14:457-464.
[129] Chalasani N, Abdelmalek MF, Garcia-Tsao G, Vuppalanchi R, Alkhouri N, Rinella M, et al. Effects of Belapectin, an Inhibitor of Galectin-3, in Patients With Nonalcoholic Steatohepatitis With Cirrhosis and Portal Hypertension. Gastroenterology 2020;158:1334-1345.e1335.
[130] Luangmonkong T, Suriguga S, Bigaeva E, Boersema M, Oosterhuis D, de Jong KP, et al. Evaluating the antifibrotic potency of galunisertib in a human ex vivo model of liver fibrosis. Br J Pharmacol 2017;174:3107-3117.
[131] Hui ST, Wang F, Stappenbeck F, French SW, Magyar CE, Parhami F, et al. Oxy210, a novel inhibitor of hedgehog and TGF-β signalling, ameliorates hepatic fibrosis and hypercholesterolemia in mice. Endocrinol Diabetes Metab 2021;4:e00296.
[132] Marra F, Tacke F. Roles for chemokines in liver disease. Gastroenterology 2014;147:577-594.e571.
[133] Gimeno RE, Briere DA, Seeley RJ. Leveraging the Gut to Treat Metabolic Disease. Cell Metab 2020;31:679-698.
[134] Liu Y, Wei R, Hong TP. Potential roles of glucagon-like peptide-1-based therapies in treating non-alcoholic fatty liver disease. World J Gastroenterol 2014;20:9090-9097.
[135] Young AA, Gedulin BR, Bhavsar S, Bodkin N, Jodka C, Hansen B, et al. Glucose-lowering and insulin-sensitizing actions of exendin-4: studies in obese

diabetic (ob/ob, db/db) mice, diabetic fatty Zucker rats, and diabetic rhesus monkeys (Macaca mulatta). Diabetes 1999;48:1026-1034.
[136] Armstrong MJ, Hull D, Guo K, Barton D, Hazlehurst JM, Gathercole LL, et al. Glucagon-like peptide 1 decreases lipotoxicity in non-alcoholic steatohepatitis. J Hepatol 2016;64:399-408.
[137] Newsome PN, Buchholtz K, Cusi K, Linder M, Okanoue T, Ratziu V, et al. A Placebo-Controlled Trial of Subcutaneous Semaglutide in Nonalcoholic Steatohepatitis. N Engl J Med 2021;384:1113-1124.
[138] Ala M. SGLT2 Inhibition for Cardiovascular Diseases, Chronic Kidney Disease, and NAFLD. Endocrinology 2021;162.
[139] Tahara A, Takasu T, Yokono M, Imamura M, Kurosaki E. Characterization and comparison of SGLT2 inhibitors: Part 3. Effects on diabetic complications in type 2 diabetic mice. Eur J Pharmacol 2017;809:163-171.
[140] Liao CJ, Huang PS, Chien HT, Lin TK, Yeh CT, Lin KH. Effects of Thyroid Hormones on Lipid Metabolism Pathologies in Non-Alcoholic Fatty Liver Disease. Biomedicines 2022;10.
[141] Sinha RA, Bruinstroop E, Singh BK, Yen PM. Nonalcoholic Fatty Liver Disease and Hypercholesterolemia: Roles of Thyroid Hormones, Metabolites, and Agonists. Thyroid 2019;29:1173-1191.
[142] Krause C, Grohs M, El Gammal AT, Wolter S, Lehnert H, Mann O, et al. Reduced expression of thyroid hormone receptor β in human nonalcoholic steatohepatitis. Endocr Connect 2018;7:1448-1456.
[143] Perra A, Kowalik MA, Cabras L, Runfola M, Sestito S, Migliore C, et al. Potential role of two novel agonists of thyroid hormone receptor-β on liver regeneration. Cell Prolif 2020;53:e12808.
[144] Trost SU, Swanson E, Gloss B, Wang-Iverson DB, Zhang H, Volodarsky T, et al. The thyroid hormone receptor-beta-selective agonist GC-1 differentially affects plasma lipids and cardiac activity. Endocrinology 2000;141:3057-3064.
[145] Martagón AJ, Lin JZ, Cimini SL, Webb P, Phillips KJ. The amelioration of hepatic steatosis by thyroid hormone receptor agonists is insufficient to restore insulin sensitivity in ob/ob mice. PLoS One 2015;10:e0122987.
[146] Perra A, Simbula G, Simbula M, Pibiri M, Kowalik MA, Sulas P, et al. Thyroid hormone (T3) and TRbeta agonist GC-1 inhibit/reverse nonalcoholic fatty liver in rats. FASEB J 2008;22:2981-2989.
[147] Wang X, Wang L, Geng L, Tanaka N, Ye B. Resmetirom Ameliorates NASH-Model Mice by Suppressing STAT3 and NF-κB Signaling Pathways in an RGS5-Dependent Manner. Int J Mol Sci 2023;24.
[148] Kelly MJ, Pietranico-Cole S, Larigan JD, Haynes NE, Reynolds CH, Scott N, et al. Discovery of 2-[3,5-dichloro-4-(5-isopropyl-6-oxo-1,6-dihydropyridazin-3-yloxy)phenyl]-3,5-dioxo-2,3,4,5-tetrahydro[1,2,4]triazine-6-carbonitrile (MGL-3196), a Highly Selective Thyroid Hormone Receptor β agonist in clinical trials for the treatment of dyslipidemia. J Med Chem 2014;57:3912-3923.
[149] Harrison SA, Bashir M, Moussa SE, McCarty K, Pablo Frias J, Taub R, et al. Effects of Resmetirom on Noninvasive Endpoints in a 36-Week Phase 2 Active Treatment Extension Study in Patients With NASH. Hepatol Commun 2021;5:573-588.
[150] Harrison SA, Bashir MR, Guy CD, Zhou R, Moylan CA, Frias JP, et al. Resmetirom (MGL-3196) for the treatment of non-alcoholic steatohepatitis: a multicentre, randomised, double-blind, placebo-controlled, phase 2 trial. Lancet 2019;394:2012-2024.
[151] Ma Q. Role of nrf2 in oxidative stress and toxicity. Annu Rev Pharmacol Toxicol 2013;53:401-426.
[152] Yamamoto M, Kensler TW, Motohashi H. The KEAP1-NRF2 System: a Thiol-Based Sensor-Effector Apparatus for Maintaining Redox Homeostasis. Physiol Rev 2018;98:1169-1203.

[153] Suzuki T, Motohashi H, Yamamoto M. Toward clinical application of the Keap1-Nrf2 pathway. Trends Pharmacol Sci 2013;34:340-346.
[154] Dinkova-Kostova AT, Abramov AY. The emerging role of Nrf2 in mitochondrial function. Free Radic Biol Med 2015;88:179-188.
[155] Segmen MYaH. Two Faces of Nrf2 in Cancer. 2022.
[156] Fukai T, Ushio-Fukai M. Superoxide dismutases: role in redox signaling, vascular function, and diseases. Antioxid Redox Signal 2011;15:1583-1606.
[157] Yasui K, Baba A. Therapeutic potential of superoxide dismutase (SOD) for resolution of inflammation. Inflamm Res 2006;55:359-363.
[158] Koruk M, Taysi S, Savas MC, Yilmaz O, Akcay F, Karakok M. Oxidative stress and enzymatic antioxidant status in patients with nonalcoholic steatohepatitis. Ann Clin Lab Sci 2004;34:57-62.
[159] Świderska M, Maciejczyk M, Zalewska A, Pogorzelska J, Flisiak R, Chabowski A. Oxidative stress biomarkers in the serum and plasma of patients with non-alcoholic fatty liver disease (NAFLD). Can plasma AGE be a marker of NAFLD? Oxidative stress biomarkers in NAFLD patients. Free Radic Res 2019;53:841-850.
[160] Djordjević VV, Kostić J, Krivokapić Ž, Krtinić D, Ranković M, Petković M, et al. Decreased Activity of Erythrocyte Catalase and Glutathione Peroxidase in Patients with Schizophrenia. Medicina (Kaunas) 2022;58.
[161] Chan JY, Chan SH. Activation of endogenous antioxidants as a common therapeutic strategy against cancer, neurodegeneration and cardiovascular diseases: A lesson learnt from DJ-1. Pharmacol Ther 2015;156:69-74.
[162] Nishinaka Y, Nakamura H, Masutani H, Yodoi J. Redox control of cellular function by thioredoxin; a new therapeutic direction in host defence. Arch Immunol Ther Exp (Warsz) 2001;49:285-292.
[163] Powis G, Montfort WR. Properties and biological activities of thioredoxins. Annu Rev Biophys Biomol Struct 2001;30:421-455.
[164] Monteiro HP, Ogata FT, Stern A. Thioredoxin promotes survival signaling events under nitrosative/oxidative stress associated with cancer development. Biomed J 2017;40:189-199.
[165] Chen C, Wang K, Zhang H, Zhou HJ, Chen Y, Min W. A Unique SUMO-Interacting Motif of Trx2 Is Critical for Its Mitochondrial Presequence Processing and Anti-oxidant Activity. Front Physiol 2019;10:1089.
[166] Shu N, Hägglund P, Cai H, Hawkins CL, Davies MJ. Modification of Cys residues in human thioredoxin-1 by p-benzoquinone causes inhibition of its catalytic activity and activation of the ASK1/p38-MAPK signalling pathway. Redox Biol 2020;29:101400.
[167] Sun QA, Su D, Novoselov SV, Carlson BA, Hatfield DL, Gladyshev VN. Reaction mechanism and regulation of mammalian thioredoxin/glutathione reductase. Biochemistry 2005;44:14528-14537.
[168] Arnér ES, Holmgren A. Physiological functions of thioredoxin and thioredoxin reductase. Eur J Biochem 2000;267:6102-6109.
[169] Zhong L, Arnér ES, Holmgren A. Structure and mechanism of mammalian thioredoxin reductase: the active site is a redox-active selenolthiol/selenenylsulfide formed from the conserved cysteine-selenocysteine sequence. Proc Natl Acad Sci U S A 2000;97:5854-5859.
[170] Collet JF, Messens J. Structure, function, and mechanism of thioredoxin proteins. Antioxid Redox Signal 2010;13:1205-1216.
[171] Karlenius TC, Tonissen KF. Thioredoxin and Cancer: A Role for Thioredoxin in all States of Tumor Oxygenation. Cancers (Basel) 2010;2:209-232.
[172] Wu M, Deng C, Lo TH, Chan KY, Li X, Wong CM. Peroxiredoxin, Senescence, and Cancer. Cells 2022;11.
[173] Marks PA. Thioredoxin in cancer--role of histone deacetylase inhibitors. Semin Cancer Biol 2006;16:436-443.
[174] Husbeck B, Powis G. The redox protein thioredoxin-1 regulates the constitutive and inducible expression of the estrogen metabolizing cytochromes P450

1B1 and 1A1 in MCF-7 human breast cancer cells. Carcinogenesis 2002;23:1625-1630.
[175] Bhatia M, McGrath KL, Di Trapani G, Charoentong P, Shah F, King MM, et al. The thioredoxin system in breast cancer cell invasion and migration. Redox Biol 2016;8:68-78.
[176] Kakolyris S, Giatromanolaki A, Koukourakis M, Powis G, Souglakos J, Sivridis E, et al. Thioredoxin expression is associated with lymph node status and prognosis in early operable non-small cell lung cancer. Clin Cancer Res 2001;7:3087-3091.
[177] Shang W, Xie Z, Lu F, Fang D, Tang T, Bi R, et al. Increased Thioredoxin-1 Expression Promotes Cancer Progression and Predicts Poor Prognosis in Patients with Gastric Cancer. Oxid Med Cell Longev 2019;2019:9291683.
[178] Samaranayake GJ, Troccoli CI, Huynh M, Lyles RDZ, Kage K, Win A, et al. Thioredoxin-1 protects against androgen receptor-induced redox vulnerability in castration-resistant prostate cancer. Nat Commun 2017;8:1204.
[179] Sumida Y, Nakashima T, Yoh T, Furutani M, Hirohama A, Kakisaka Y, et al. Serum thioredoxin levels as a predictor of steatohepatitis in patients with nonalcoholic fatty liver disease. J Hepatol 2003;38:32-38.
[180] Schumacker PT. Reactive oxygen species in cancer cells: live by the sword, die by the sword. Cancer Cell 2006;10:175-176.
[181] Paz MM, Zhang X, Lu J, Holmgren A. A new mechanism of action for the anticancer drug mitomycin C: mechanism-based inhibition of thioredoxin reductase. Chem Res Toxicol 2012;25:1502-1511.
[182] Zhou J, Chng WJ. Roles of thioredoxin binding protein (TXNIP) in oxidative stress, apoptosis and cancer. Mitochondrion 2013;13:163-169.
[183] Saxena G, Chen J, Shalev A. Intracellular shuttling and mitochondrial function of thioredoxin-interacting protein. J Biol Chem 2010;285:3997-4005.
[184] Zhou J, Bi C, Cheong LL, Mahara S, Liu SC, Tay KG, et al. The histone methyltransferase inhibitor, DZNep, up-regulates TXNIP, increases ROS production, and targets leukemia cells in AML. Blood 2011;118:2830-2839.
[185] Saadati S, Sadeghi A, Mansour A, Yari Z, Poustchi H, Hedayati M, et al. Curcumin and inflammation in non-alcoholic fatty liver disease: a randomized, placebo controlled clinical trial. BMC Gastroenterol 2019;19:133.
[186] Ngu MH, Norhayati MN, Rosnani Z, Zulkifli MM. Curcumin as adjuvant treatment in patients with non-alcoholic fatty liver (NAFLD) disease: A systematic review and meta-analysis. Complement Ther Med 2022;68:102843.
[187] Heger M. Drug screening: Don't discount all curcumin trial data. Nature 2017;543:40.
[188] Rodriguez-Garcia A, Hevia D, Mayo JC, Gonzalez-Menendez P, Coppo L, Lu J, et al. Thioredoxin 1 modulates apoptosis induced by bioactive compounds in prostate cancer cells. Redox Biol 2017;12:634-647.
[189] Li GZ, Liang HF, Liao B, Zhang L, Ni YA, Zhou HH, et al. PX-12 inhibits the growth of hepatocelluar carcinoma by inducing S-phase arrest, ROS-dependent apoptosis and enhances 5-FU cytotoxicity. Am J Transl Res 2015;7:1528-1540.
[190] Yu T, Tang B, Sun X. Development of Inhibitors Targeting Hypoxia-Inducible Factor 1 and 2 for Cancer Therapy. Yonsei Med J 2017;58:489-496.
[191] Carvalho CM, Lu J, Zhang X, Arnér ES, Holmgren A. Effects of selenite and chelating agents on mammalian thioredoxin reductase inhibited by mercury: implications for treatment of mercury poisoning. FASEB J 2011;25:370-381.
[192] Prast-Nielsen S, Cebula M, Pader I, Arnér ES. Noble metal targeting of thioredoxin reductase--covalent complexes with thioredoxin and thioredoxin-related protein of 14 kDa triggered by cisplatin. Free Radic Biol Med 2010;49:1765-1778.
[193] Wataha JC, Lewis JB, McCloud VV, Shaw M, Omata Y, Lockwood PE, et al. Effect of mercury(II) on Nrf2, thioredoxin reductase-1 and thioredoxin-1 in human monocytes. Dent Mater 2008;24:765-772.

[194] Jurgens S, Kuhn FE, Casini A. Cyclometalated Complexes of Platinum and Gold with Biological Properties: State-of-the-Art and Future Perspectives. Curr Med Chem 2018;25:437-461.
[195] Sasada T, Nakamura H, Ueda S, Sato N, Kitaoka Y, Gon Y, et al. Possible involvement of thioredoxin reductase as well as thioredoxin in cellular sensitivity to cis-diamminedichloroplatinum (II). Free Radic Biol Med 1999;27:504-514.
[196] Gandin V, Fernandes AP, Rigobello MP, Dani B, Sorrentino F, Tisato F, et al. Cancer cell death induced by phosphine gold(I) compounds targeting thioredoxin reductase. Biochem Pharmacol 2010;79:90-101.
[197] Roder C, Thomson MJ. Auranofin: repurposing an old drug for a golden new age. Drugs R D 2015;15:13-20.
[198] Oh BM, Lee SJ, Cho HJ, Park YS, Kim JT, Yoon SR, et al. Cystatin SN inhibits auranofin-induced cell death by autophagic induction and ROS regulation via glutathione reductase activity in colorectal cancer. Cell Death Dis 2017;8:e2682.
[199] Hou GX, Liu PP, Zhang S, Yang M, Liao J, Yang J, et al. Elimination of stem-like cancer cell side-population by auranofin through modulation of ROS and glycolysis. Cell Death Dis 2018;9:89.
[200] You BR, Park WH. Auranofin induces mesothelioma cell death through oxidative stress and GSH depletion. Oncol Rep 2016;35:546-551.
[201] Fhu CW, Ali A. Dysregulation of the Ubiquitin Proteasome System in Human Malignancies: A Window for Therapeutic Intervention. Cancers (Basel) 2021;13.
[202] Lee SM, Koh DH, Jun DW, Roh YJ, Kang HT, Oh JH, et al. Auranofin attenuates hepatic steatosis and fibrosis in nonalcoholic fatty liver disease via NRF2 and NF- κB signaling pathways. Clin Mol Hepatol 2022;28:827-840.
[203] Hwangbo H, Kim MY, Ji SY, Kim SY, Lee H, Kim GY, et al. Auranofin Attenuates Non-Alcoholic Fatty Liver Disease by Suppressing Lipid Accumulation and NLRP3 Inflammasome-Mediated Hepatic Inflammation In Vivo and In Vitro. Antioxidants (Basel) 2020;9.
[204] Dowman JK, Tomlinson JW, Newsome PN. Pathogenesis of non-alcoholic fatty liver disease. Qjm 2010;103:71-83.
[205] Zeilinger K, Freyer N, Damm G, Seehofer D, Knöspel F. Cell sources for in vitro human liver cell culture models. Exp Biol Med (Maywood) 2016;241:1684-1698.
[206] Ramboer E, Vanhaecke T, Rogiers V, Vinken M. Immortalized Human Hepatic Cell Lines for In Vitro Testing and Research Purposes. Methods Mol Biol 2015;1250:53-76.
[207] Nikolic M, Sustersic T, Filipovic N. Models and On-Chip Systems: Biomaterial Interaction Studies With Tissues Generated Using Lung Epithelial and Liver Metabolic Cell Lines. Front Bioeng Biotechnol 2018;6:120.
[208] López-Terrada D, Cheung SW, Finegold MJ, Knowles BB. Hep G2 is a hepatoblastoma-derived cell line. Hum Pathol 2009;40:1512-1515.
[209] Guengerich FP. Cytochrome P450 research and. J Biol Chem 2019;294:1671-1680.
[210] Westerink WM, Schoonen WG. Cytochrome P450 enzyme levels in HepG2 cells and cryopreserved primary human hepatocytes and their induction in HepG2 cells. Toxicol In Vitro 2007;21:1581-1591.
[211] Seo JE, Tryndyak V, Wu Q, Dreval K, Pogribny I, Bryant M, et al. Quantitative comparison of in vitro genotoxicity between metabolically competent HepaRG cells and HepG2 cells using the high-throughput high-content CometChip assay. Arch Toxicol 2019;93:1433-1448.
[212] Guo Y, Cai X, Lu H, Li Q, Zheng Y, Lin Z, et al. 17β-Estradiol Promotes Apoptosis of HepG2 Cells Caused by Oxidative Stress by Increasing Foxo3a Phosphorylation. Front Pharmacol 2021;12:607379.
[213] Bai X, Hong W, Cai P, Chen Y, Xu C, Cao D, et al. Valproate induced hepatic steatosis by enhanced fatty acid uptake and triglyceride synthesis. Toxicol Appl Pharmacol 2017;324:12-25.

[214] Donato MT, Tolosa L, Gómez-Lechón MJ. Culture and Functional Characterization of Human Hepatoma HepG2 Cells. Methods Mol Biol 2015;1250:77-93.
[215] Chavez-Tapia NC, Rosso N, Tiribelli C. Effect of intracellular lipid accumulation in a new model of non-alcoholic fatty liver disease. BMC Gastroenterol 2012;12:20.
[216] Gunn PJ, Pramfalk C, Millar V, Cornfield T, Hutchinson M, Johnson EM, et al. Modifying nutritional substrates induces macrovesicular lipid droplet accumulation and metabolic alterations in a cellular model of hepatic steatosis. Physiol Rep 2020;8:e14482.
[217] Guillouzo A, Corlu A, Aninat C, Glaise D, Morel F, Guguen-Guillouzo C. The human hepatoma HepaRG cells: a highly differentiated model for studies of liver metabolism and toxicity of xenobiotics. Chem Biol Interact 2007;168:66-73.
[218] Deng J, Wei W, Chen Z, Lin B, Zhao W, Luo Y, et al. Engineered Liver-on-a-Chip Platform to Mimic Liver Functions and Its Biomedical Applications: A Review. Micromachines (Basel) 2019;10.
[219] Doktorova TY, Yildirimman R, Vinken M, Vilardell M, Vanhaecke T, Gmuender H, et al. Transcriptomic responses generated by hepatocarcinogens in a battery of liver-based in vitro models. Carcinogenesis 2013;34:1393-1402.
[220] Bell CC, Lauschke VM, Vorrink SU, Palmgren H, Duffin R, Andersson TB, et al. Transcriptional, Functional, and Mechanistic Comparisons of Stem Cell-Derived Hepatocytes, HepaRG Cells, and Three-Dimensional Human Hepatocyte Spheroids as Predictive In Vitro Systems for Drug-Induced Liver Injury. Drug Metab Dispos 2017;45:419-429.
[221] Alkhatatbeh MJ, Lincz LF, Thorne RF. Low simvastatin concentrations reduce oleic acid-induced steatosis in HepG(2) cells: An in vitro model of non-alcoholic fatty liver disease. Exp Ther Med 2016;11:1487-1492.
[222] Khalifa O, K HM, Mall R, Ullah E, N SA-A, Arredouani A. Investigation of the Effect of Exendin-4 on Oleic Acid-Induced Steatosis in HepG2 Cells Using Fourier Transform Infrared Spectroscopy. Biomedicines 2022;10.
[223] Cui W, Chen SL, Hu KQ. Quantification and mechanisms of oleic acid-induced steatosis in HepG2 cells. Am J Transl Res 2010;2:95-104.
[224] Wang Y, Parlevliet ET, Geerling JJ, van der Tuin SJ, Zhang H, Bieghs V, et al. Exendin-4 decreases liver inflammation and atherosclerosis development simultaneously by reducing macrophage infiltration. Br J Pharmacol 2014;171:723-734.
[225] Swapna Sasi US, Sindhu G, Raghu KG. Fructose-palmitate based high calorie induce steatosis in HepG2 cells via mitochondrial dysfunction: An in vitro approach. Toxicol In Vitro 2020;68:104952.
[226] Justo R, Boada J, Frontera M, Oliver J, Bermúdez J, Gianotti M. Gender dimorphism in rat liver mitochondrial oxidative metabolism and biogenesis. Am J Physiol Cell Physiol 2005;289:C372-378.
[227] Stirone C, Duckles SP, Krause DN, Procaccio V. Estrogen increases mitochondrial efficiency and reduces oxidative stress in cerebral blood vessels. Mol Pharmacol 2005;68:959-965.
[228] Galmés-Pascual BM, Nadal-Casellas A, Bauza-Thorbrügge M, Sbert-Roig M, García-Palmer FJ, Proenza AM, et al. 17β-estradiol improves hepatic mitochondrial biogenesis and function through PGC1B. J Endocrinol 2017;232:297-308.
[229] Farruggio S, Cocomazzi G, Marotta P, Romito R, Surico D, Calamita G, et al. Genistein and 17β-Estradiol Protect Hepatocytes from Fatty Degeneration by Mechanisms Involving Mitochondria, Inflammasome and Kinases Activation. Cell Physiol Biochem 2020;54:401-416.
[230] Gupta R, Schrooders Y, Hauser D, van Herwijnen M, Albrecht W, Ter Braak B, et al. Comparing in vitro human liver models to in vivo human liver using RNA-Seq. Arch Toxicol 2021;95:573-589.

[231] Sharma S, Mells JE, Fu PP, Saxena NK, Anania FA. GLP-1 analogs reduce hepatocyte steatosis and improve survival by enhancing the unfolded protein response and promoting macroautophagy. PLoS One 2011;6:e25269.
[232] Wobser H, Dorn C, Weiss TS, Amann T, Bollheimer C, Büttner R, et al. Lipid accumulation in hepatocytes induces fibrogenic activation of hepatic stellate cells. Cell Res 2009;19:996-1005.
[233] Baze A, Parmentier C, Hendriks DFG, Hurrell T, Heyd B, Bachellier P, et al. Three-Dimensional Spheroid Primary Human Hepatocytes in Monoculture and Coculture with Nonparenchymal Cells. Tissue Eng Part C Methods 2018;24:534-545.
[234] Seidemann L, Krüger A, Kegel-Hübner V, Seehofer D, Damm G. Influence of Genistein on Hepatic Lipid Metabolism in an In Vitro Model of Hepatic Steatosis. Molecules 2021;26.
[235] Kozyra M, Johansson I, Nordling Å, Ullah S, Lauschke VM, Ingelman-Sundberg M. Human hepatic 3D spheroids as a model for steatosis and insulin resistance. Sci Rep 2018;8:14297.
[236] Kostrzewski T, Cornforth T, Snow SA, Ouro-Gnao L, Rowe C, Large EM, et al. Three-dimensional perfused human in vitro model of non-alcoholic fatty liver disease. World J Gastroenterol 2017;23:204-215.
[237] Aoudjehane L, Gautheron J, Le Goff W, Goumard C, Gilaizeau J, Nget CS, et al. Novel defatting strategies reduce lipid accumulation in primary human culture models of liver steatosis. Dis Model Mech 2020;13.
[238] Cai J, Chen J, Liu Y, Miura T, Luo Y, Loring JF, et al. Assessing self-renewal and differentiation in human embryonic stem cell lines. Stem Cells 2006;24:516-530.
[239] Trounson A. The production and directed differentiation of human embryonic stem cells. Endocr Rev 2006;27:208-219.
[240] Steiner D, Khaner H, Cohen M, Even-Ram S, Gil Y, Itsykson P, et al. Derivation, propagation and controlled differentiation of human embryonic stem cells in suspension. Nat Biotechnol. United States; 2010. p. 361-364.
[241] Fernandez Tde S, de Souza Fernandez C, Mencalha AL. Human induced pluripotent stem cells from basic research to potential clinical applications in cancer. Biomed Res Int 2013;2013:430290.
[242] Timilsina S, Kirsch-Mangu T, Werth S, Shepard B, Ma T, Villa-Diaz LG. Enhanced self-renewal of human pluripotent stem cells by simulated microgravity. NPJ Microgravity 2022;8:22.
[243] Lu J, Einhorn S, Venkatarangan L, Miller M, Mann DA, Watkins PB, et al. Morphological and Functional Characterization and Assessment of iPSC-Derived Hepatocytes for In Vitro Toxicity Testing. Toxicol Sci 2015;147:39-54.
[244] Szkolnicka D, Farnworth SL, Lucendo-Villarin B, Hay DC. Deriving functional hepatocytes from pluripotent stem cells. Curr Protoc Stem Cell Biol 2014;30:1g.5.1-12.
[245] Sinton MC, Meseguer-Ripolles J, Lucendo-Villarin B, Wernig-Zorc S, Thomson JP, Carter RN, et al. A human pluripotent stem cell model for the analysis of metabolic dysfunction in hepatic steatosis. iScience 2021;24:101931.
[246] Muñoz A, Theusch E, Kuang YL, Nalula G, Peaslee C, Dorlhiac G, et al. Undifferentiated Induced Pluripotent Stem Cells as a Genetic Model for Nonalcoholic Fatty Liver Disease. Cell Mol Gastroenterol Hepatol 2022;14:1174-1176.e1176.
[247] Graffmann N, Ncube A, Martins S, Fiszl AR, Reuther P, Bohndorf M, et al. A stem cell based in vitro model of NAFLD enables the analysis of patient specific individual metabolic adaptations in response to a high fat diet and AdipoRon interference. Biol Open 2021;10.
[248] Soret PA, Magusto J, Housset C, Gautheron J. In Vitro and In Vivo Models of Non-Alcoholic Fatty Liver Disease: A Critical Appraisal. J Clin Med 2020;10.
[249] Sinton MC, Meseguer-Ripolles J, Lucendo-Villarin B, Drake AJ, Hay DC. Modeling human hepatic steatosis in pluripotent stem cell-derived hepatocytes. STAR Protoc 2021;2:100493.

[250] Zhang R, Chu K, Zhao N, Wu J, Ma L, Zhu C, et al. Corilagin Alleviates Nonalcoholic Fatty Liver Disease in High-Fat Diet-Induced C57BL/6 Mice by Ameliorating Oxidative Stress and Restoring Autophagic Flux. Front Pharmacol 2019;10:1693.
[251] Lyall MJ, Cartier J, Thomson JP, Cameron K, Meseguer-Ripolles J, O'Duibhir E, et al. Modelling non-alcoholic fatty liver disease in human hepatocyte-like cells. Philos Trans R Soc Lond B Biol Sci 2018;373.
[252] Cruz ALS, Barreto EA, Fazolini NPB, Viola JPB, Bozza PT. Lipid droplets: platforms with multiple functions in cancer hallmarks. Cell Death Dis 2020;11:105.
[253] Motomura W, Inoue M, Ohtake T, Takahashi N, Nagamine M, Tanno S, et al. Up-regulation of ADRP in fatty liver in human and liver steatosis in mice fed with high fat diet. Biochem Biophys Res Commun 2006;340:1111-1118.
[254] Palierne G, Fabre A, Solinhac R, Le Péron C, Avner S, Lenfant F, et al. Changes in Gene Expression and Estrogen Receptor Cistrome in Mouse Liver Upon Acute E2 Treatment. Mol Endocrinol 2016;30:709-732.
[255] Rooney J, Oshida K, Vasani N, Vallanat B, Ryan N, Chorley BN, et al. Activation of Nrf2 in the liver is associated with stress resistance mediated by suppression of the growth hormone-regulated STAT5b transcription factor. PLoS One 2018;13:e0200004.
[256] Deroo BJ, Hewitt SC, Peddada SD, Korach KS. Estradiol regulates the thioredoxin antioxidant system in the mouse uterus. Endocrinology 2004;145:5485-5492.
[257] May HC, Yu JJ, Guentzel MN, Chambers JP, Cap AP, Arulanandam BP. Repurposing Auranofin, Ebselen, and PX-12 as Antimicrobial Agents Targeting the Thioredoxin System. Front Microbiol 2018;9:336.
[258] Subudhi S, Drescher HK, Dichtel LE, Bartsch LM, Chung RT, Hutter MM, et al. Distinct Hepatic Gene-Expression Patterns of NAFLD in Patients With Obesity. Hepatol Commun 2022;6:77-89.
[259] Ramos MJ, Bandiera L, Menolascina F, Fallowfield JA. models for non-alcoholic fatty liver disease: Emerging platforms and their applications. iScience 2022;25:103549.
[260] Long F, Bhatti MR, Kellenberger A, Sun W, Modica S, Höring M, et al. A low-carbohydrate diet induces hepatic insulin resistance and metabolic associated fatty liver disease in mice. Mol Metab 2023;69:101675.
[261] Phan H, Richard A, Lazo M, Nelson WG, Denmeade SR, Groopman J, et al. The association of sex steroid hormone concentrations with non-alcoholic fatty liver disease and liver enzymes in US men. Liver Int 2021;41:300-310.
[262] Fuller KNZ, McCoin CS, Von Schulze AT, Houchen CJ, Choi MA, Thyfault JP. Estradiol treatment or modest exercise improves hepatic health and mitochondrial outcomes in female mice following ovariectomy. Am J Physiol Endocrinol Metab 2021;320:E1020-E1031.
[263] Zhu L, Shi J, Luu TN, Neuman JC, Trefts E, Yu S, et al. Hepatocyte estrogen receptor alpha mediates estrogen action to promote reverse cholesterol transport during Western-type diet feeding. Mol Metab 2018;8:106-116.
[264] Morselli E, Santos RS, Gao S, Ávalos Y, Criollo A, Palmer BF, et al. Impact of estrogens and estrogen receptor-α in brain lipid metabolism. Am J Physiol Endocrinol Metab 2018;315:E7-E14.
[265] Carr MC. The emergence of the metabolic syndrome with menopause. J Clin Endocrinol Metab 2003;88:2404-2411.
[266] Song CH, Kim N, Kim DH, Lee HN, Surh YJ. 17-β estradiol exerts anti-inflammatory effects through activation of Nrf2 in mouse embryonic fibroblasts. PLoS One 2019;14:e0221650.
[267] Hima S, Sreeja S. Regulatory role of estrogen-induced reactive oxygen species in the modulatory function of UCP 2 in papillary thyroid cancer cells. IUBMB Life 2015;67:837-846.

[268] Maleki J, Nourbakhsh M, Shabani M, Korani M, Nourazarian SM, Ostadali Dahaghi MR, et al. 17β-Estradiol Stimulates Generation of Reactive Species Oxygen and Nitric Oxide in Ovarian Adenocarcinoma Cells (OVCAR 3). Iran J Cancer Prev 2015;8:e2332.
[269] Kövesdi E, Szabó-Meleg E, Abrahám IM. The Role of Estradiol in Traumatic Brain Injury: Mechanism and Treatment Potential. Int J Mol Sci 2020;22.
[270] Onodera T, Momose I, Kawada M. Potential Anticancer Activity of Auranofin. Chem Pharm Bull (Tokyo) 2019;67:186-191.
[271] Smiriglia A, Lorito N, Serra M, Perra A, Morandi A, Kowalik MA. Sex difference in liver diseases: How preclinical models help to dissect the sex-related mechanisms sustaining NAFLD and hepatocellular carcinoma. iScience 2023;26:108363.
[272] Freire Boullosa L, Van Loenhout J, Hermans C, Lau HW, Merlin C, Marcq E, et al. Optimization of the Solvent and In Vivo Administration Route of Auranofin in a Syngeneic Non-Small Cell Lung Cancer and Glioblastoma Mouse Model. Pharmaceutics 2022;14.